DOT/FAA/TC-20/10

Federal Aviation Administration
William J. Hughes Technical Center
Aviation Research Division
Atlantic City International Airport
New Jersey 08405

Safer Lithium-ion Battery Development with Reduced Flammability Electrolyte

Owen Crowther, Logan Wittmaier, James Bond, Mario Destephen

May 2020

Final Report

U.S. Department of Transportation
Federal Aviation Administration

NOTICE

Technical Report Documentation Page

1. Report No.	2. Government Accession No.	3. Recipient's Catalog No.
DOT/FAA/TC-20/10		

4. Title and Subtitle	5. Report Date
Safer Lithium-ion Battery Development with Reduced Flammability Electrolyte	May 2020
	6. Performing Organization Code
7. Author(s)	8. Performing Organization Report No.
Owen Crowther, Logan Wittmaier, James Bond, Mario Destephen	
9. Performing Organization Name and Address	10. Work Unit No. (TRAIS)
EaglePicher Technologies P.O. Box 47 Joplin MO 64802-004	11. Contract or Grant No. DTFACT-16-C-00043
12. Sponsoring Agency Name and Address	13. Type of Report and Period Covered
AAQ-610 Facilities & Grants FAA William J. Hughes Technical Center Building 300, Fourth Floor Atlantic City International Airport Atlantic City NJ 08405	Final Report February 2017 – November 2019
	14. Sponsoring Agency Code AAQ610-AFN

15. Supplementary Notes

16. Abstract

Improving the safety of Li-ion batteries for aircraft applications has been addressed by demonstrating a technical approach of layered mitigations to reduce the effect of cell thermal runaway. A reduced flammability electrolyte is shown to eliminate or reduce venting of Li-ion cells during overdischarge, external short circuit, and overheating, while also shown to have equal or better performance compared to standard cells at temperatures from -30° Celsius to +50° Celsius. Non-flammable coatings are demonstrated to eliminate or reduce combustion of battery components otherwise caused by ignition of cell vent products. Full 7P2S Li-ion battery modules are tested to DO-311A protocols for overdischarge, external short circuit, and overheating, without experiencing evidence of flame or fire. Test controls to demonstrate the improved design compared to conventional Li-ion cells and battery assembly methods were performed with 7P2S battery modules fabricated with conventional Li-ion cells and without the benefit of flame-retardant battery design. Those control tests showed that severe venting and fire were caused by the DO-311A abuse tests. This project provides encouraging evidence that the safety of Li-ion batteries can be improved through reduced flammability electrolytes and flame-retardant materials. Continued refinement of this approach may enable existing and new safety-critical applications for industries such as aircraft and aerospace.

17. Key Words	18. Distribution Statement
lithium, lithium-ion, battery, thermal runaway, reduced flammability	No restrictions. This document is available to the U.S. public through the National Technical Information Service (NTIS), Springfield, Virginia 22161. This document is also available from the Federal Aviation Administration William J. Hughes Technical Center at actlibrary.tc.faa.gov.

19. Security Classif. (of this report)	20. Security Classif. (of this page)	21. No. of Pages	22. Price
Unclassified	Unclassified	82	

Form DOT F 1700.7 (8-72) Reproduction of completed page authorized

TABLE OF CONTENTS

LIST OF FIGURES

LIST OF TABLES

LIST OF ACRONYMS

Ah	Ampere-hour
ARC	Accelerating Rate Calorimeter
BL	Baseline
BMS	Battery Management System
DSC	Differential Scanning Calorimetry
FAA	Federal Aviation Administration
JAA	Joint Aviation Authority
LFP	Lithium Iron Phosphate
Li-ion	Lithium-ion
MOPS	Minimum Operational Performance Standard
NCM	Nickel Cobalt Manganese Oxide
PTC	Positive Temperature Coefficient
RF	Reduced Flammability
RT	Room Temperature
RTCA	Radio Technical Commission for Aeronautics
S-FHA	System Functional Hazard Assessment
S.E.T.	Self-Extinguishing Time
SEI	Solid Electrolyte Interphase
SoC	State of Charge
Wh	Watt-hour
xPyS	y Blocks in Series of x Cells in Parallel

EXECUTIVE SUMMARY

EaglePicher previously developed a reduced flammability (RF) electrolyte to improve safety of Lithium-ion (Li-ion) batteries. During this project, the RF electrolyte was optimized and integrated into 26650 cells with Lithium Iron Phosphate (LFP) cathode. The same electrolyte also was tested with higher-energy Nickel Cobalt Manganese Oxide (NCM) cathodes in prototype 18650 cells. NCM improved the specific energy and energy density without compromising safety. The new RF cells were to be incorporated into an existing aircraft battery design to demonstrate the improved safety of the battery when subjected to the failure aspects of DO-311A, and the preceding FAA Memorandum ANM-113-10-004.

The RF electrolyte was formulated to inhibit flame generation at the cell level to prevent thermal runaway. The RF electrolyte showed better stability, lower heat generation, and lower flammability than a baseline (BL) electrolyte in *ex situ* tests. Performance and abuse tests conducted on both NCM-based 18650 cells and LFP-based 26650 cells demonstrated that the use of RF electrolyte produced improved safety without compromising performance. The 18650 cells activated with RF electrolyte demonstrated similar rate and temperature capability as BL cells. The 26650 LFP cells with these electrolytes demonstrated similar capacity up to 8C rates through a temperature range of −30 to +50 °C. Cells using RF electrolyte demonstrated better abuse tolerance in all safety tests. No cells with the RF electrolyte caught fire, while several cells with the BL electrolyte did.

Flame-retardant coatings were also evaluated to mitigate thermal events and demonstrated reduced flammability. Most test cases resulted in localized charring and no sustained flame. The coatings were either sprayed on a porous fabric incorporated in the battery design or painted on the interior of the battery case.

Originally, a third component of the overall cell-failure mitigation plan was to develop a carbon fiber, post-suppressant material. This material development effort had hoped to directly address cell emissions that may result from venting (with or without thermal runaway present) that could result in a secondary fire, or a larger resulting failure event. Unfortunately, due to contractual difficulties with the intended technology initiator, EaglePicher was unable to pursue this complementary technology. As an alternative, EaglePicher proposed, as an amendment to the original contract, to include a detailed chemical and physical analysis of resulting failed-cell emissions.

Accelerated rate calorimetry (ARC) testing collected data on both pressure and temperature-rise rates for BL and RF cells under thermal runaway. This data was used to construct ANSYS simulations of the battery submodule under the same thermal runaway conditions. These simulations indicated a significantly longer time to venting temperatures for RF batteries.

Battery level overcharge, overheating and short-circuit tests were conducted on 7P2S batteries to compare BL cells to RF electrolyte cells with incorporated flame retardants. RF batteries led to fewer vented cells and no evidence of fire after testing. BL batteries showed large-scale and violent venting in the overheating and short-circuit tests with evidence of fire. EaglePicher was able to create a significantly safer Li-ion battery that provides encouraging examples for future development of Li-ion batteries in aviation and other industries.

1. INTRODUCTION

Li-ion battery performance has become enabling for the many mobile and cordless devices that have become commonplace in modern society. Its original high-specific energy and energy density has been further developed to provide even higher energy and power densities, making it attractive not only for the early uses such as cell phones and laptop computers, but also for large high-discharge batteries applicable to installation on aircraft.

However, batteries typically become more susceptible to uncontrolled energy releases as energy densities increase, and Li-ion is no exception. Various abuse conditions produce energy release that cannot be absorbed or transferred out of the battery, resulting in rapid temperature rise. High internal temperatures increase reactivity of components, leading to exothermic reactions, which, in turn, produce a thermal runaway and pressure rise, causing the cell to vent flammable organic electrolytes. The heat of a single failing cell can cause adjacent cells to fail, propagating through the battery. Reactive cell components can also provide an ignition source to the venting electrolyte, resulting in a fire that can cause secondary combustion of other battery components.

In an effort to mitigate the problems of Li-ion fires and catastrophic failure, EaglePicher previously developed electrolytes with RF. These RF electrolytes have been applied to aircraft battery development compliant to the DO-311 Minimum Operational Performance Standard (MOPS). These batteries employ a layered safety design to significantly reduce the probability of a catastrophic failure resulting from the thermal runaway. This report addresses the further development of a safer Li-ion battery by reducing both the probability of cell venting and the combustion of other battery components.

Demonstration of an RF electrolyte in the cell was accomplished, providing supporting test data for compliance with the regulatory requirements and performance specifications applicable to aircraft applications of Li-ion batteries. The proprietary RF electrolyte formulation was developed by optimizing the electrolyte salt and solvent formulation, while also selecting suitable fire-retardant additive(s) to support the required cell performance and improving safety. To avoid secondary combustion of other battery components, flame-retardant coatings were investigated to mitigate propagation of thermal runaway and ignition of other battery components.

The challenge in developing a practical RF electrolyte required overcoming the negative effect a fire-retardant additive can have on cell discharge rate and low-temperature capabilities. Several fire-retardant additives—such as fluorinated solvents, phosphate, phosphonate, phosphite, bisphenol-A, and organosilicon—have demonstrated fire-retardant capability, but also led to reductions in discharge-rate capability with degraded cycle life performance [1]. EaglePicher's optimized RF electrolyte was able to produce the required performance while providing safety advantages in Li-ion batteries.

2. METHODOLOGY

The ability of an improved RF electrolyte to replace the BL electrolyte with minimal performance impact while increasing safety was evaluated in *ex situ* tests. The down-selected RF electrolyte was incorporated into cells to evaluate performance and safety compared to BL characteristics. Flame retardant coatings were evaluated to characterize their abilities to slow or stop propagation of flames in the presence of cells undergoing thermal runaway. Data from these tests was used to produce an ANSYS simulation to predict the effects on battery-level safety testing. Finally, battery submodule safety tests were conducted with cells containing the RF electrolyte and flame-retardant coatings. These tests were compared with submodules built with BL electrolyte cells and no flame-retardant coating to demonstrate the improved safety of this combined approach.

3. ELECTROLYTE AND CELL TESTING

Performance and safety characteristics of the two electrolytes, RF and BL, were evaluated in three test categories:

- Electrolyte stability tests include voltage stability window between 5 volts and 0.01 volts; exothermic decomposition using differential scanning calorimetry (DSC); exothermic reactions of electrodes cycled in the two electrolytes using DSC; and voltage and thermal stability
- Electrolyte performance tests include rate and temperature characterization of each electrolyte in 18650 and 26650 cells
- Electrolyte safety evaluation includes DO-311A abuse tests on 26650 cells at room temperature overcharge, 55° C overcharge, overheating to force venting with an ignition source present, and external short circuit at 55° C

3.1 ELECTROLYTE CHARACTERIZATION

The improved RF electrolyte was developed by blending a flame-retardant additive in a mixture of carbonate solvents. Formulations containing high amounts of flame-retardant additive improve the safety at the cost of rate capability and low-temperature performance [1]. The amount of flame-retardant was optimized to enable reduced flammability while maintaining cell performance [2]. The BL electrolyte used for comparison is a widely used conventional carbonate electrolyte. Figure 1 shows a cyclic voltammetry experiment that compares the electrochemical stability of RF and BL electrolyte. The voltage was scanned between 5 and 0.01 V at a 1 mV s^{-1} rate with a blocking working electrode and a lithium counter electrode. The RF electrolyte demonstrated similar voltage stability in the operational voltage window of 4.3 to 2 V.

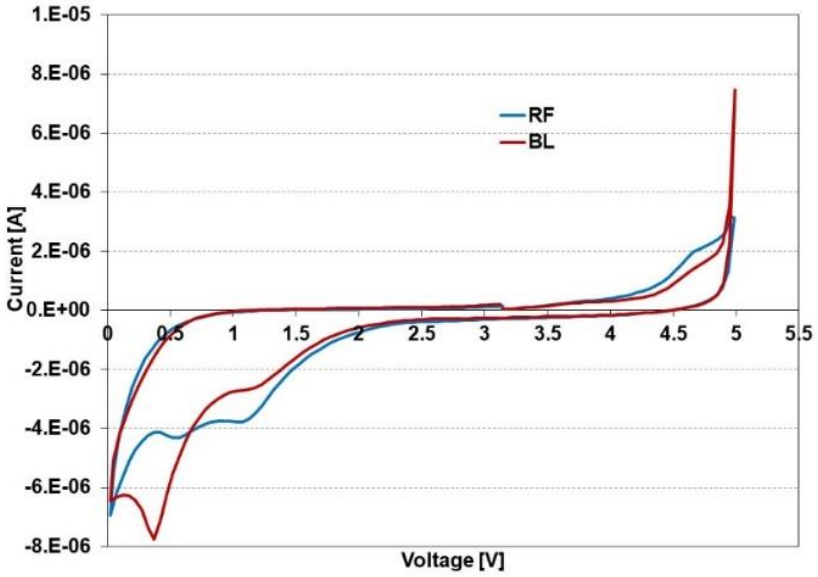

Figure 1. Cyclic voltammogram of BL and RF electrolyte @ 1mV/s

Differential scanning calorimetry (DSC) evaluations of RF and BL electrolytes were conducted in a nitrogen atmosphere using a Netzsch Maia 200 F3 DSC instrument. Figure 2 shows the RF-electrolyte, exothermic decomposition reaction shifted to a higher temperature and the heat output was lower than the BL electrolyte. Table 1 summarizes the DSC data.

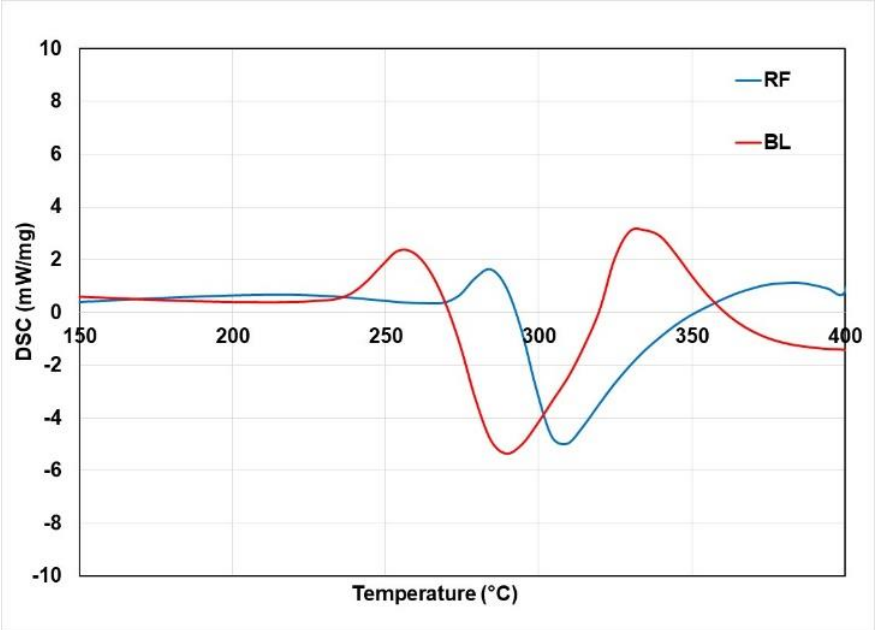

Figure 2. DSC of RF vs BL electrolytes

Table 1. Electrolyte DSC characterization

Electrolyte	Peak (°C)	Heat ($J\ g^{-1}$)
BL	288	1050
RF	308	754

Thermal stability of the electrode/electrolyte interface was further investigated using cycled half-cells made with NCM cathode or graphite anode containing RF and BL electrolytes. The cells were charged and discharged three times at a C/10 rate, and stopped at the most thermally unstable state of the tested electrode. The cells were opened inside an argon-filled glove box and the electrodes were removed from the cycled cell for DSC analysis. Table 2 shows that delithiated NCM released 50% less exothermic heat with RF electrolyte. Delithiated LFP showed very little heat generation with both electrolytes because of its relatively higher thermal stability.

Table 2. Summary of DSC data of delithiated cathodes & lithiated anode

Material	Exothermic Heat ($J\ g^{-1}$)	
	BL	RF
Delithiated NCM	3770	2207
Delithiated LFP	319	308
Lithiated Anode	465	302

The anode solid electrolyte interphase (SEI) decomposition involves a series of reactions leading to thermal runaway. The total heat generation from all anode SEI layer decomposition reactions is lower for the RF electrolyte compared to the BL electrolyte. This demonstrates an improved anode SEI layer stability with RF electrolyte.

Figure 3 shows open-cup flammability tests that demonstrate the reduced flammability of RF electrolyte compared to the BL in the presence of a flame. While the BL electrolyte caught on fire in the presence of the flame, the RF electrolyte did not.

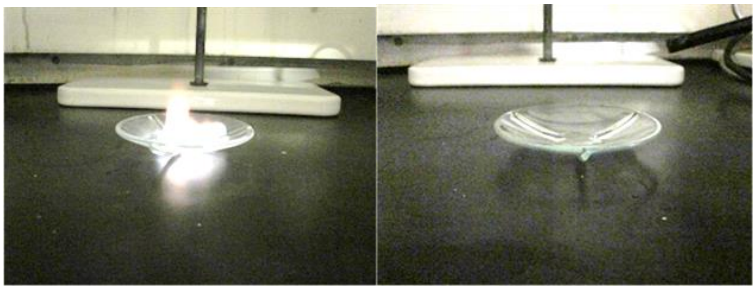

Figure 3. Flammability tests of BL (left) and RF (right) electrolytes

Each analysis indicates a significantly improved RF electrolyte with lower heat generation and reduced flammability compared to the BL electrolyte. This electrolyte was then used in cylindrical cells to demonstrate improved safety while maintaining performance.

3.2 CYLINDRICAL CELL DISCHARGE CHARACTERIZATION

Two Ah prototype 18650 cells were made using a standard NCM-based cathode, graphite anode and trilayer separator. Cells were activated with both BL and RF electrolytes. Cell formation was performed using our standard procedure. Figure 4 shows the rate capability of these cells after formation. Cells with the RF electrolyte demonstrate similar capacity to the 1C rate.

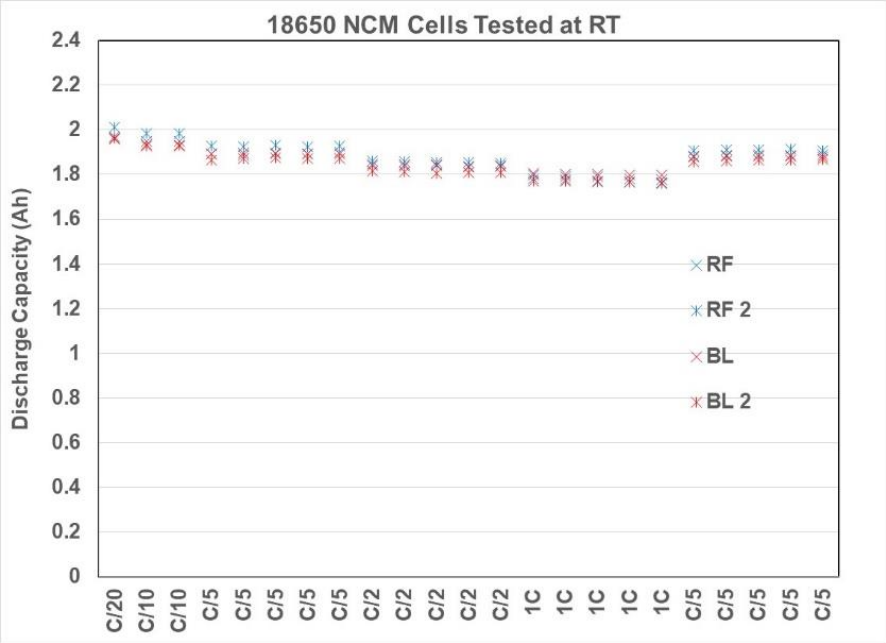

Figure 4. Capacity of NCM-based 18650 cells

Figure 5 shows the rate capability of 2.5 Ah 26650 LFP cells currently used in EaglePicher's aircraft batteries. Cells with the RF and BL electrolyte deliver similar capacity to an 8C rate.

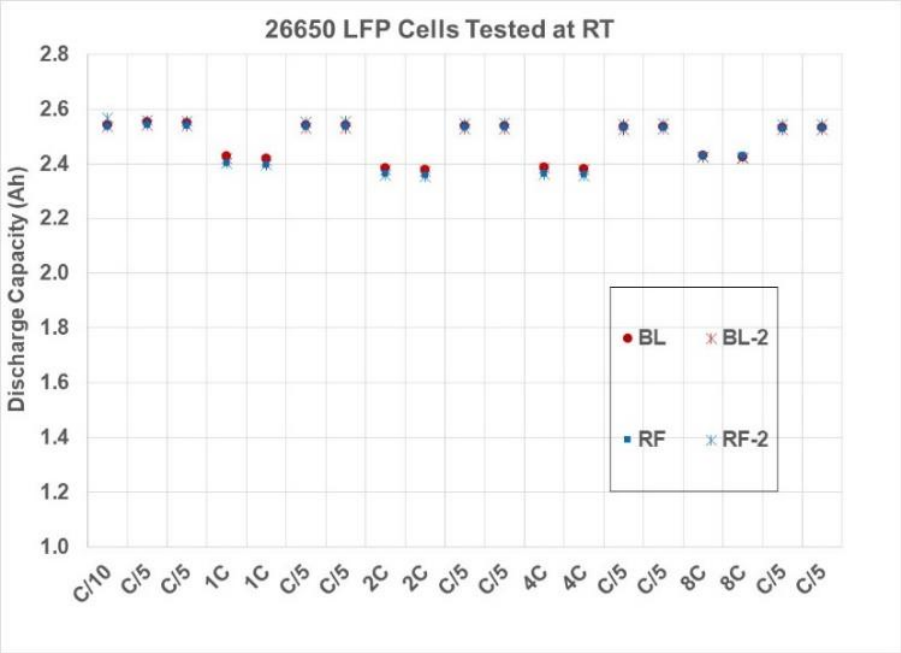

Figure 5. Capacity of LFP-based 26650 cells

Figure 6Figure 6 shows 26650s with RF and BL electrolytes demonstrate similar discharge voltages and skin temperatures, indicating that the RF electrolyte did not increase impedance.

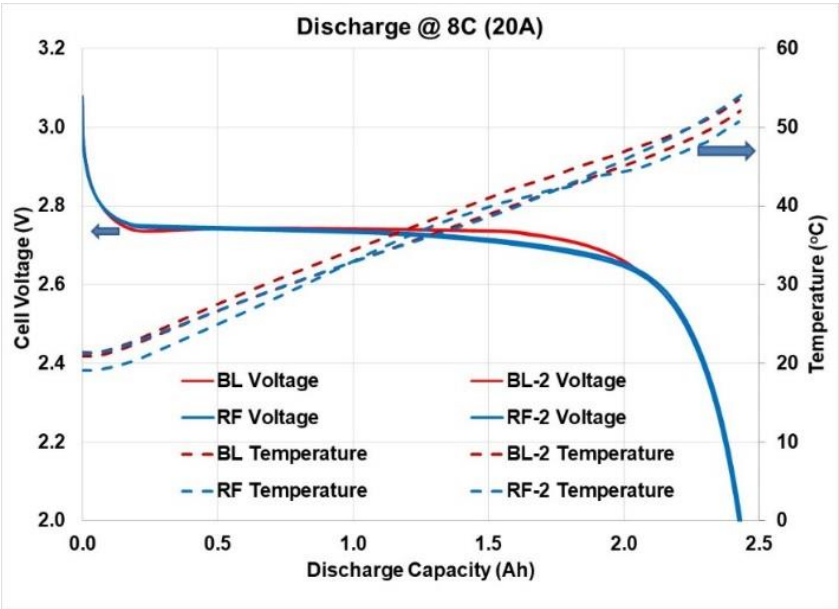

Figure 6. Temperature & discharge profile of 26650 LFP cells at 8C rate

Figure 7 shows 26650 LFP cells tested at different temperatures. The cells were discharged at 1C for all temperatures except −30°C. Cells at −30°C were discharged at C/20 and demonstrated higher capacity when using the RF electrolyte. 26650s with the RF and BL demonstrated similar capacities from −20 to 50°C. Figure 8 and Figure 9 show the voltage profile during discharge.

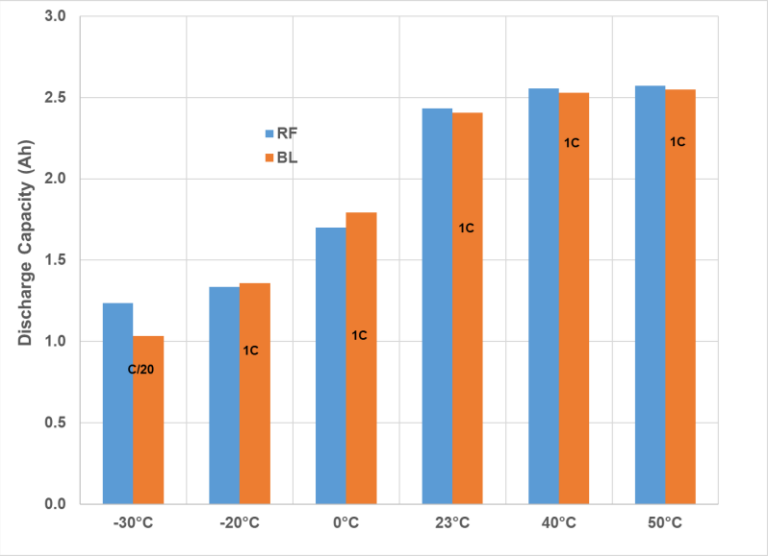

Figure 7. Summary of 26650 LFP cells tested at different rates from -30°C to +50°C

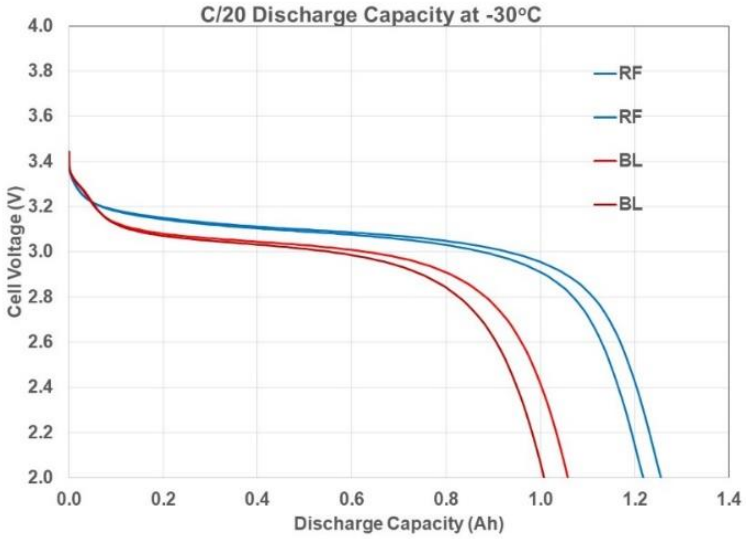

Figure 8. 26650 LFP cell voltage profile at −30°C

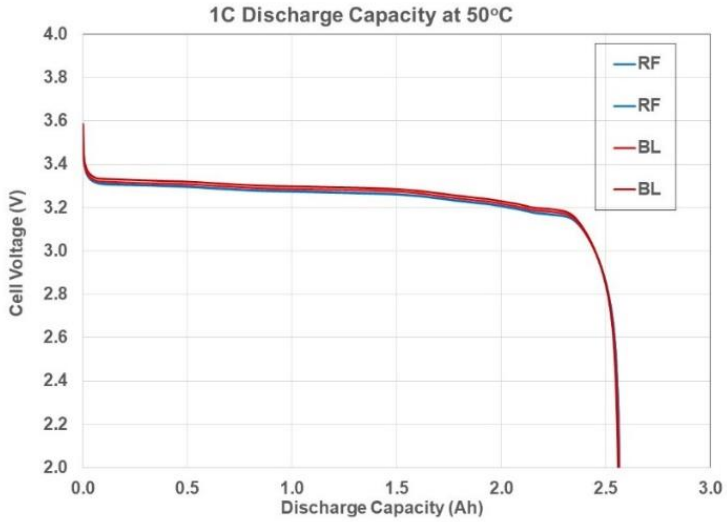

Figure 9. 26650 LFP cell voltage profile at 50°C

These tests demonstrate the RF electrolyte does not decrease the rate capability or cold temperature performance of the cells.

3.3 SAFETY TESTS IN LFP 26650 CELLS

EaglePicher performed several safety tests on 26650 cells with LFP cathode and RF or BL electrolyte (shown in Table 3). The cells were formed using standard procedures. All cells were charged to 100% state-of-charge (SoC) before safety testing. The cells were then tested according to the procedures described below.

Table 3. Summary of safety tests on LFP 26650 cells

Electrolyte type	Abuse Test	Result	Skin (°C)	Header/ Vent (°C)
BL	Overcharge 20A @ RT	Vented in 2 min. **Fire**	500	NA
BL	Overcharge 20A @ 55°C	Vented in 8 min. **Jelly roll expelled with fire**	118	136
BL	Overcharge 20A @ 55°C	Vented 7.5 min. No fire but fumes	103	70
BL	Overcharge 20A @ 55°C	Vented in 10 min. **Fire**	176	179

Electrolyte type	Abuse Test	Result	Skin (°C)	Header/ Vent (°C)
BL	Overcharge 20A @ 55°C	Vented in 3 min. Jelly roll expelled	123	111
RF	Overcharge 20A @ RT	Vented in 3 min. No fire	94	NA
RF	Overcharge 20A @ RT	Vented in 3 min. No fire	89	NA
RF	Overcharge 20A @ RT	Vented in 3 min. No fire	NA	NA
RF	Overcharge 20A @ 55°C	Vented in 2 min. No fire	108	NA
RF	Overcharge 20A @ 55°C	Vented in 6min. No fire	109	72
RF	Overcharge 20A @ 55°C	Vented in 7min. No fire	115	77
RF	Overcharge 20A @ 55°C	Vented in 2 min.	103	97
BL	Overheating with spark	**Fire**	172	370
BL	Overheating with spark	**Fire** & Jelly roll expelled	172	122
RF	Overheating with spark	Venting and smoke	156	207
RF	Overheating with spark	Venting	121	153
BL	External Short @ 55°C	I_{max} 235A. **Fire**	170	N/A
RF	External Short @ 55°C	fI_{max} 72A. vented	152	N/A
RF	External Short @ 55°C	I_{max} 62A. No venting	112	N/A

The overcharge test was performed by charging the cell at 20A (based on prior work) at either RT or 55°C. The maximum skin temperature was higher for the 55°C tests. Three out of five cells with BL electrolyte caught fire. All seven of the RF electrolyte cells passed by not catching fire regardless of the temperature. The skin temperature of the RF cells was lower than the BL cells. Figure 10 and Figure 11 show the temperature and voltage profiles for these tests. These results demonstrate the benefit of RF electrolyte to reduce flammability and to improve battery safety under abusive conditions.

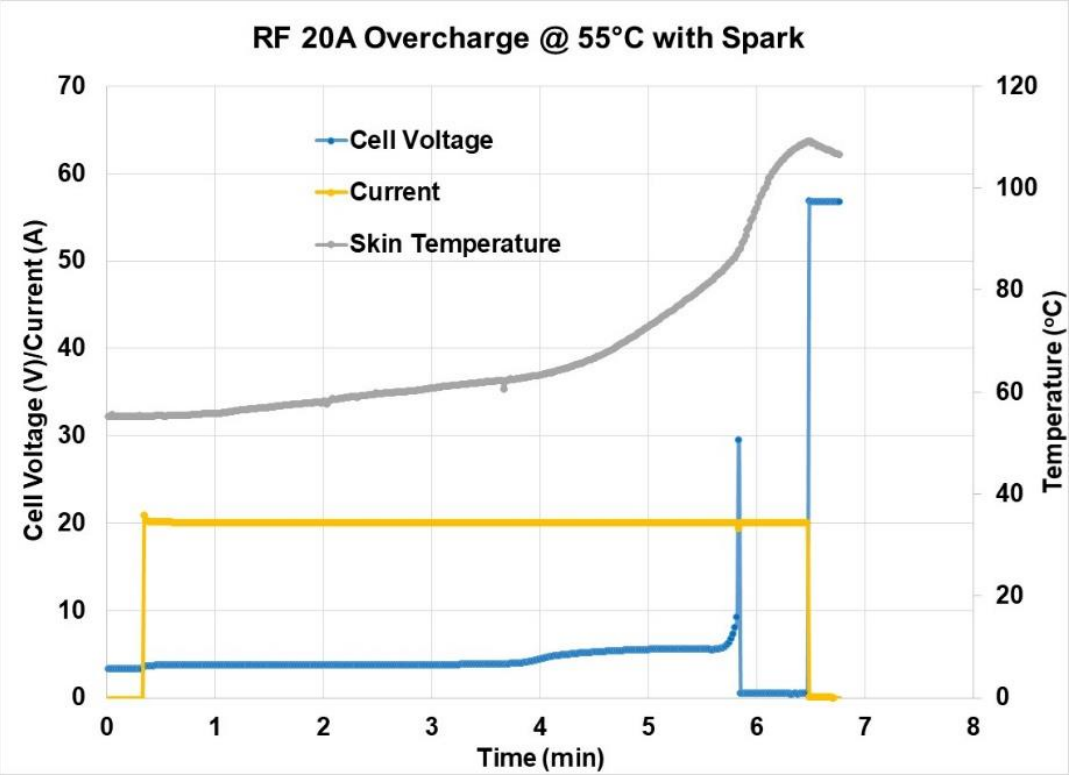

Figure 10. Overcharge test of LFP 26650 RF cells @ 55°C in the presence of a spark

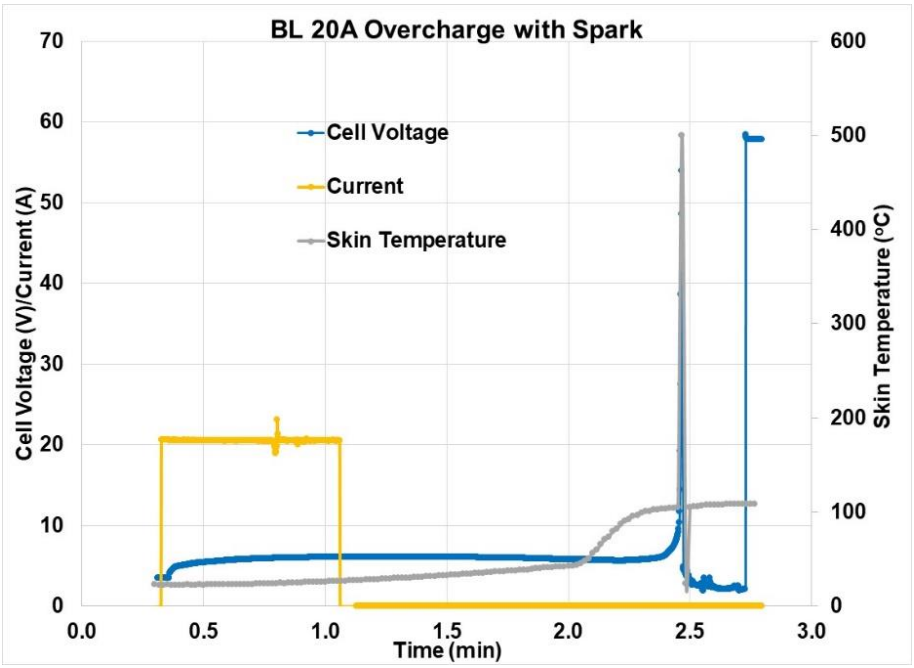

Figure 11. Overcharge test of LFP 26650 BL cells in the presence of a spark

The overheating test involved heating the cell at a rate of 5-10°C/min until the voltage dropped in the presence of a spark emitter. Figure 12 and Figure 13 show that while the cells with BL electrolyte caught fire, the RF electrolyte did not.

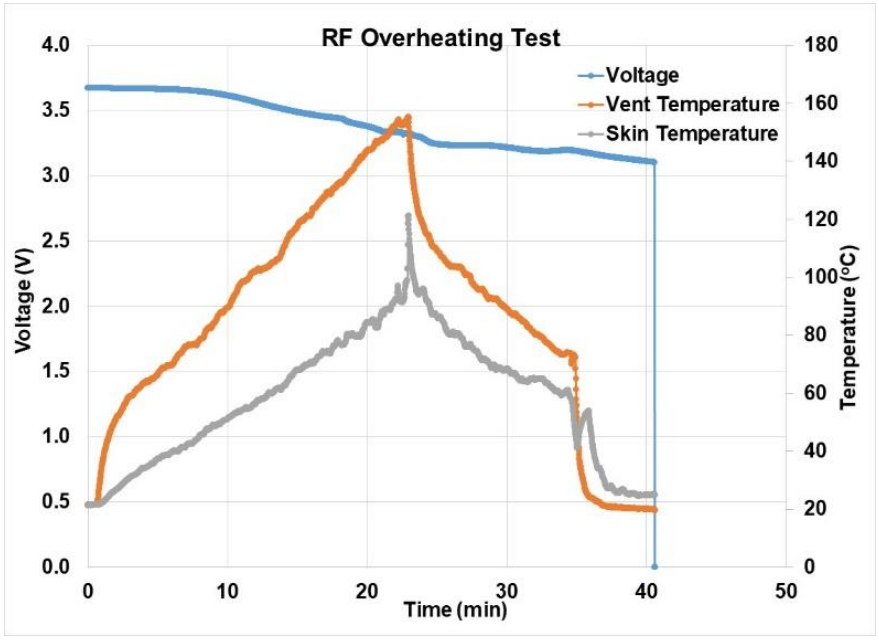

Figure 12. Overheating test of LFP 26650 RF cells in the presence of a spark

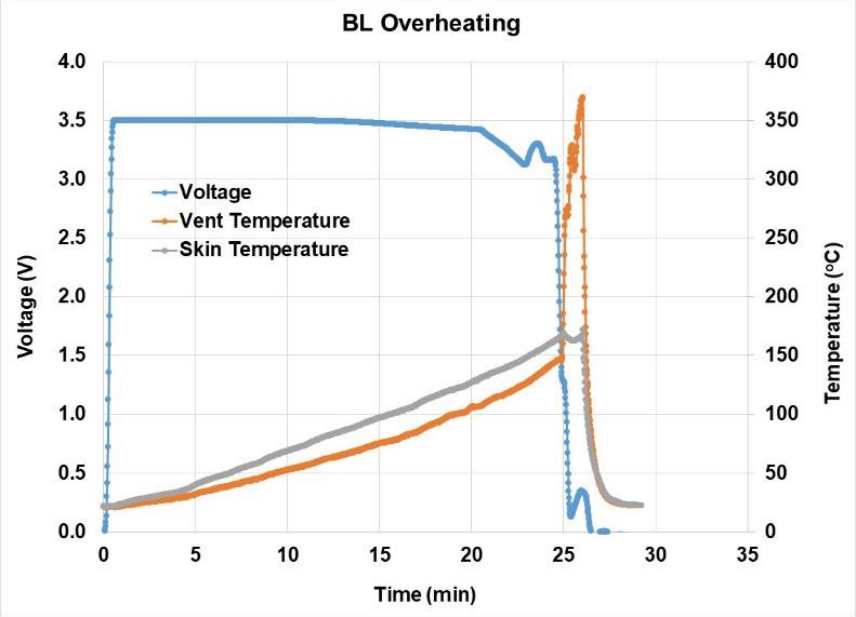

Figure 13. Overheating test of LFP 26650 BL cells in the presence of a spark

The external short test consisted of connecting a 2 mΩ resistor to the cell at 55°C. Figure 14 Figure 14and Figure 15 show the RF cell passed the test while the BL cells failed. The 26650 cells also showed a higher short current for BL (>200A) compared to RF (70A).

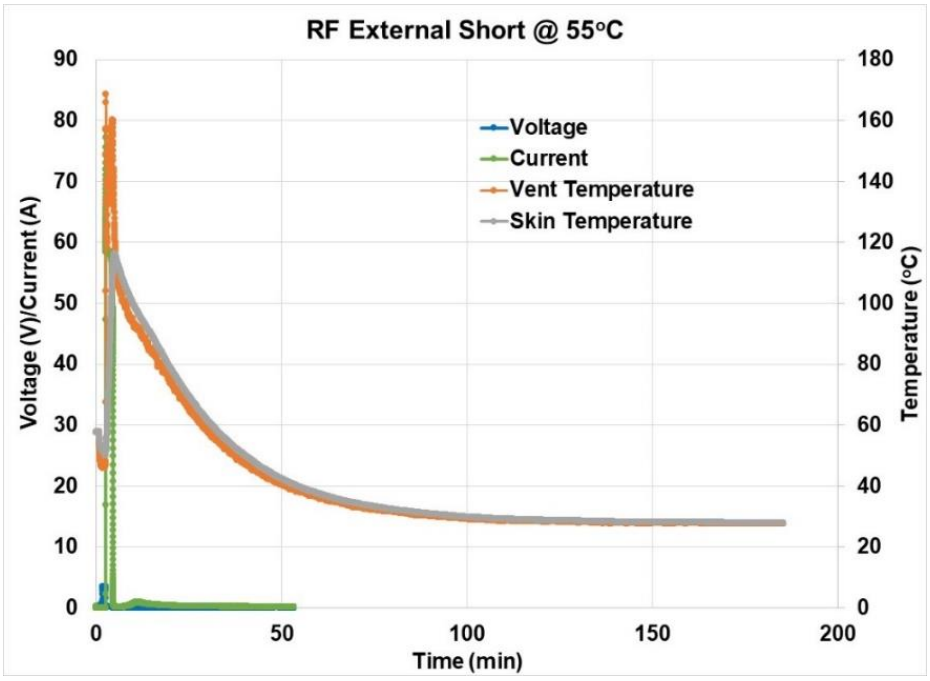

Figure 14. External short test of LFP 26650 with RF electrolyte at 55°C

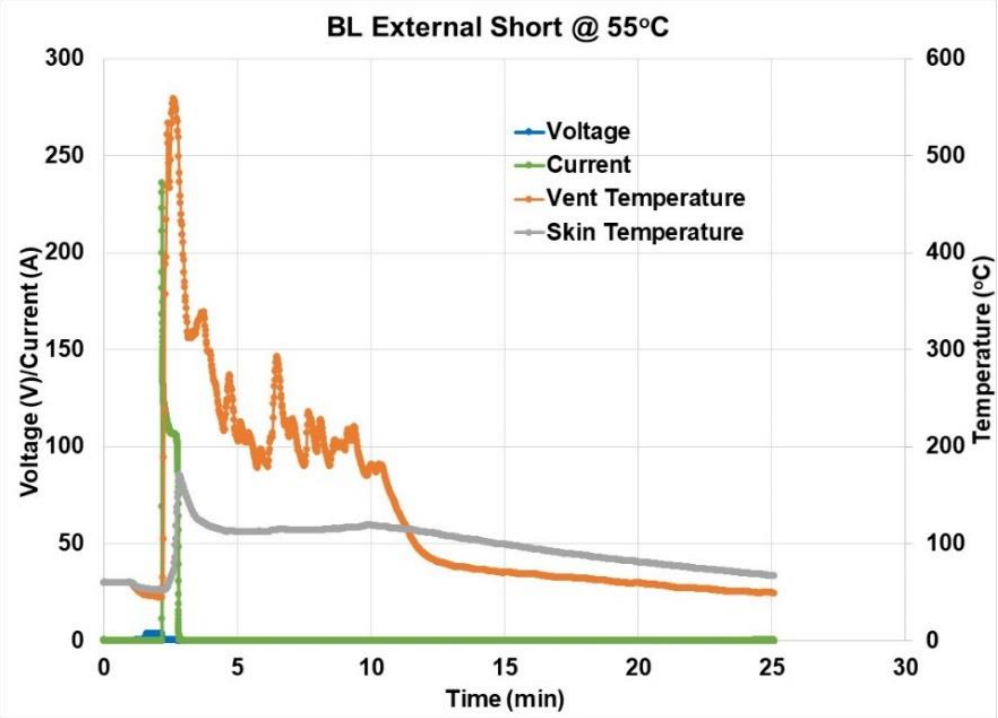

Figure 15. External short test of LFP 26650 with BL electrolyte at 55°C

3.4 ELECTROLYTE AND CELL TESTING SUMMARY

EaglePicher's aircraft batteries currently use LFP 26650s but may in the future use NCM cathode to provide higher energy. Therefore, both LFP and NCM cathodes were evaluated. Existing RF electrolyte was optimized for use with both LFP and NCM cathodes. NCM 18650s and LFP 26650s containing RF or BL electrolyte were built and subjected to performance and safety tests. The cells demonstrated no decrease in rate capability or cold temperature performance. Cells were subjected to overcharge, overheating and external short-circuit safety tests. Several cells with the BL electrolyte failed in each test. No cells with the RF electrolyte failed in any test. The RF electrolyte cells also showed lower heat generation, demonstrated by their lower temperature compared to the BL cells under similar conditions. Therefore, using the RF electrolyte in either LFP 26650s or NCM 18650s improved the cell safety while maintaining performance. Table 4 summarizes the tests as conducted under DO-311A below. The RF electrolyte improves the safety of the higher-energy NCM over that of LFP, allowing for more applications to use NCM.

Table 4. Tests conducted per RTCA/DO-311A for lithium batteries

DO-311A Test	Test Description	Results
2.4.4.5. Capacity test	Discharge the fully charged cell at Imax of the design at 23°C.	18650 NCM tested up to 1C rate and 26650 LFP tested up to 8C rate. RF and BL shows similarly good performance.
2.4.4.6. Capacity test at low and high temperatures	Discharge the fully charged cell at the Imax of the design at low and high temperatures.	26650 LFP cells were tested up to C/2 and 1C rate, respectively. RF and BL showed good performance at 1C between -20°C and 50°C. RF electrolyte cells show a better capacity than BL cells at +50°C.
2.4.5.1. Short-circuit test of a cell	External short circuit of cell at 55°C with ~2mOhm resistance.	26650 with BL failed, whereas the RF passed (see Table 3).
2.4.5.4.1. Test method for single cell thermal runaway via overcharging	Overcharging with power supply to force the cell to thermal runaway after equilibrating at temperature.	26650 cells with RF passed the test (7/7) whereas 3/5 BL cells failed (see Table 3).
2.4.5.4.2. Test method for single cell thermal runaway via overheating	Overheating at 5-10°C/min to force the cell to thermal runaway.	26650 cells made with RF (2/2) passed the test whereas the BL cells failed (see Table 3).

4. EVAULATION OF COMMERCIAL RETARDANT/SUPPRESSIVE COATINGS

EaglePicher evaluated commercial flame-retardant coatings and paints for use as additional protection within aircraft batteries. These were tested on a flammable substrate, as well as 26650 cells to evaluate their effectiveness. Thermal runaway of BL 26650 cells was initiated by overcharge to study the effectiveness of the flame-retardant materials.

4.1 MANUFACTURING METHODS AND ISSUES

Several methods were used to test the flame-retardant effectiveness of these materials. The materials were coated on Wypall paper towels, a flammable substrate material. Samples were air-dried at ambient conditions for one day before testing. Uncoated Wypall paper towels were tested as a control. All samples were exposed to a flame. Flame-retardant paint was also tested on nonporous materials like the metal battery enclosure. In general, flame-retardant sprays were coated directly on porous materials and the paints were coated on metals using a handheld paint sprayer.

4.2 PERFORMANCE TESTING DATA OF COMMERCIAL FLAME-RETARDANT MATERIALS

Table 5 shows the burn results of several flame-retardant sprays and confirms their effectiveness. Coatings A, B, and C eliminated the flammability of coated paper. Flame-retardant coating D showed lower flammability but was less effective than the first three above. These tests show that these commercial coatings are potentially useful as flame-retardant coatings within the aircraft battery.

Table 5. Summary of verification test of commercial flame-retardant coatings.

Sample	FR	Wypall mass (g)	Wypall+FR mass (g)	FR mass (g)	Burn Results
1	None	0.432	-	-	12s flame, 35s embers, smoke
2	None	0.447	-	-	12.5s flame, 38s embers, smoke
3	None	0.438	-	-	12.5s flame, 36s embers, smoke
4	FR-A	0.454	0.847	0.393	char, no smoke
5	FR-A	0.45	0.868	0.418	significant char, minimal smoke
6	FR-A	0.45	0.874	0.424	smoke, self-extinguishing flame, no embers, no burn
7	FR-B	0.443	0.78	0.337	char, minimal burn, no smoke
8	FR-B	0.451	0.797	0.346	char, minimal smoke
9	FR-B	0.439	0.798	0.359	char, smoke, minimal burn
10	FR-C	0.45	1.198	0.748	char, smoke, no burn
11	FR-C	0.444	1.077	0.633	char, smoke, no burn
12	FR-C	0.447	1.146	0.699	char, smoke, minimal burn
13	FR-D	0.448	1.117	0.669	char, smoke, burn, instantly self-extinguished flame, embers
14	FR-D	0.44	1.108	0.668	char, significant smoke, burn, instantly self-extinguished flame, embers
15	FR-D	0.448	1.239	0.791	char, smoke, burn, embers, instantly self-extinguished flame

The weathering test was then performed as a secondary screening. Each flame-retardant sample was coated on Wypalls; their masses were recorded. Samples were then stored at 70°C and 90% relative humidity for 168 hours (7 days). They were allowed to air-dry for one day, and then subjected to the flame test. Table 6 shows the results of this test.

Table 6. Summary of flame test of commercial flame-retardant coated Wypall paper towels after weathering test

S. No.	Substrate	Flame Retardant	Burn Results
1	Wypall	None	Complete Burn
2	Wypall	None	Complete Burn
3	Wypall	None	Complete Burn
4	Wypall	FR-A	Char, Smoke, Very minor deformation
5	Wypall	FR-A	Char, Smoke, Very minor deformation
6	Wypall	FR-A	Char, Smoke, Minor deformation
7	Wypall	FR-B	Char, Smoke, No ignition
8	Wypall	FR-B	Char, No ignition
9	Wypall	FR-B	Char, No ignition
10	Wypall	FR-C	Char, Smoke, No burn
11	Wypall	FR-C	Char, Smoke, Minor deformation
12	Wypall	FR-C	Char, Smoke, Minor deformation
13	Wypall	FR-D	Char, Smoke, ~10s ember
14	Wypall	FR-D	Char, Smoke, ~10s ember
15	Wypall	FR-D	Char, Smoke, ~10s ember

Flame-retardant sprays A, B, and C were found to be more effective in reducing flammability of the combustible paper based on the above tests. These materials were selected to test with an LFP 26650 under thermal runaway conditions. These tests also included a flame-retardant, paint-coated cell.

4.3 INTEGRATION PLAN AND TESTING CRITERIA

EaglePicher's aircraft battery typically consists of modules in the configuration 21P8S. The current battery also contains an insulating porous layer that wraps around the cell modules. The selected flame retardants were coated on the porous structure.

A handheld sprayer coated the flame retardants on the porous insulating layer. The samples were dried in ambient conditions. Visual observations, as well as weights of the coated sections, were used to ensure uniformity.

Cells were forced to a controlled vent condition such that gas was ejected and flame was formed from the cell header only (and not from the side or bottom of the cells). Two spark emitters and a thermocouple were placed near the header. Another thermocouple was placed on the cell surface.

4.4 TESTING WITH OVERCHARGED CELLS

Figure 16 shows the response of an LFP 26650 cell during the overcharge abuse testing without the flame-retardant coating. The cell skin and header temperatures were 120 and 270°C.

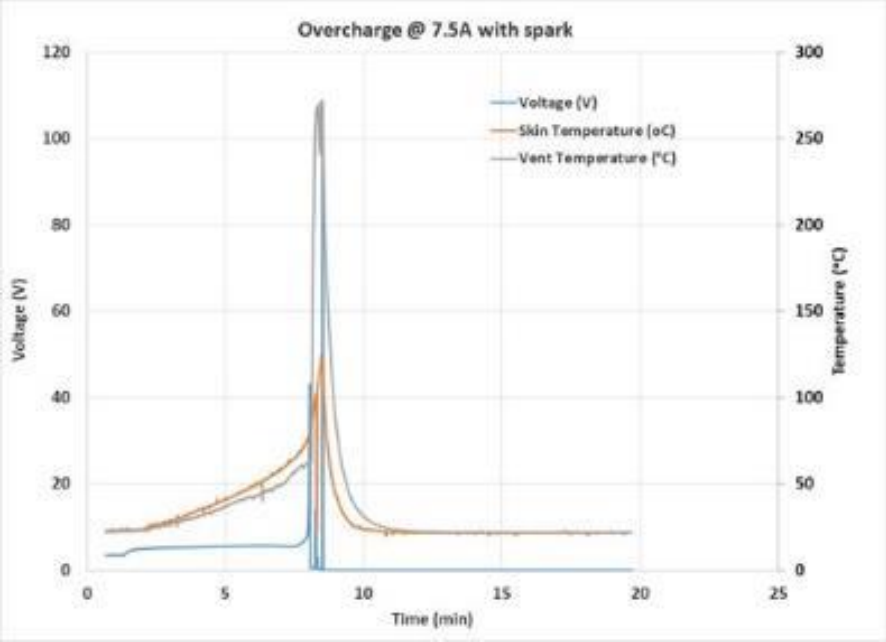

Figure 16. Overcharge test of LFP 26650 cell placed over the uncoated paper towel in the presence of a spark emitter

Figure 17 shows the same test was then repeated with the FR-A compound. The vent temperature reached 350°C and fire was observed. The paper coated with FR-A showed localized charring close to the cell header but did not catch fire. This test demonstrates the ability of FR-A to stop the propagation of fire. Tests with FR-B and FR-C demonstrated similar results.

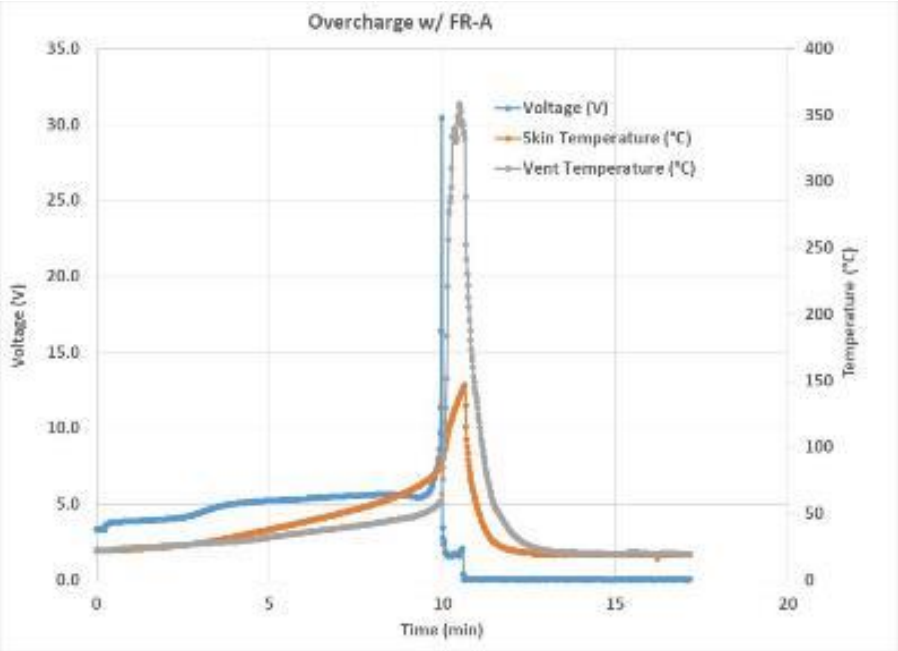

Figure 17. Overcharge test of LFP 26650 cell placed over a paper towel coated with FR-A in the presence of a spark emitter

Figure 18. Paper towel coated with FR-A did not burn, but had a localized charring when the cell went into thermal runaway in the overcharge test

Figure 19 shows the response of a LFP 26650 coated with the flame-retardant paint. The vent temperature reached more than 500°C and the skin temperature reached 180°C. Fire was observed in this test, as shown in Figure 20. Flame-retardant paint did not stop fire propagation when coated directly on the cell.

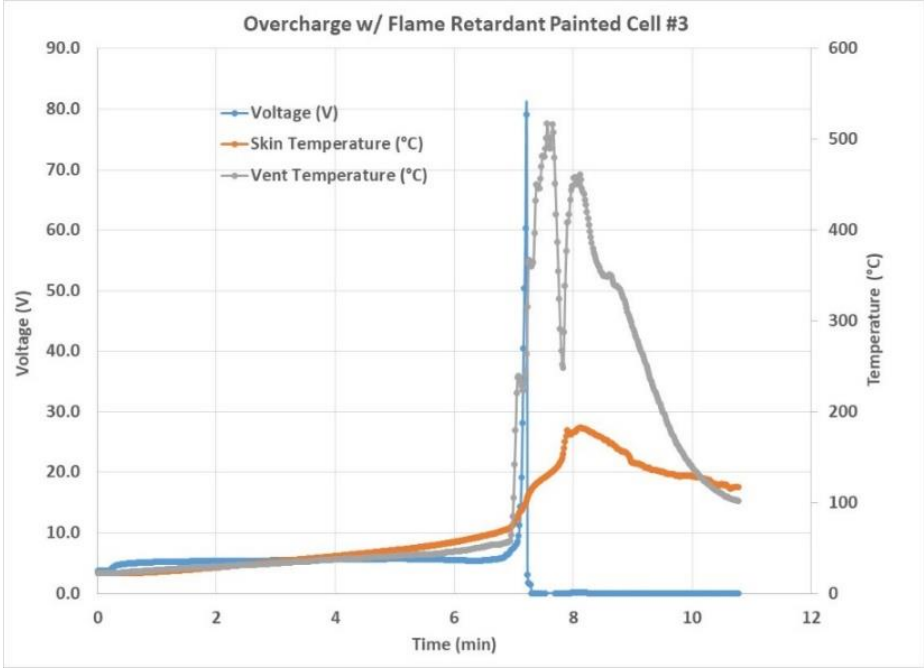

Figure 19. Overcharge test of LFP 26650 coated with a flame-retardant paint placed on an uncoated paper towel in the presence of a spark emitter

Figure 20. Flame-retardant painted LFP cell placed on an uncoated paper towel did not prevent flame propagation in the overcharge test

Figure 21 shows the result of coating the flame-retardant paint on the towel instead of the cell.

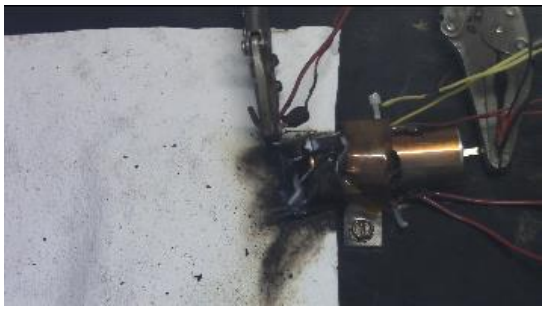

Figure 21. Paper towel coated with flame-retardant paint did not burn, despite the complete burning of the LFP cell during thermal runaway in the overcharge test

Table 7 summarizes the tests previously described. Propagation of flames is stopped by coating porous substrates surrounding the cell with flame-retardant materials. However, it is not slowed when the flame-retardant material is coated directly on the cell.

Table 7. Summary of overcharge tests of LFP 26650 cells with and without flame-retardant coatings

Flame Retardant	Result of Overcharge Test of LFP 26650 Cell	Cell T (°C)	Header T (°C)
None	Electrolyte leaked in 7mins, electrolyte and Wypall caught fire, cell blew up @7min 50s	125	272
Paper coated with FR-A1	Electrolyte leaked in 8min 29s and vent popped, electrolyte did not catch fire	N/A	N/A
Paper coated with FR-A2	Electrolyte caught fire @7:07, Wypall did not catch fire, cell blew up @ 8:14	147	358
Paper coated with FR-A3	Electrolyte leaked @8:33, Electrolyte caught fire, vent popped, Wypall didn't catch fire	165	551
Paper coated with FR-B1	Electrolyte leaked and vent popped @23.23, Electrolyte caught fire Wypall did not	381	561
Paper coated with FR-B2	Electrolyte leaked @9:48 & caught fire, Wypall didn't, cell blew up	134	279
Paper coated with FR-B3	Electrolyte leaked @8:47 & caught fire, Wypall didn't, cell blew up	117	255
Paper coated with FR-C1	Electrolyte leaked @9:08 & caught fire, Wypall didn't, cell blew up	147	358
Paper coated with FR-C2	Electrolyte leaked @7:53 & caught fire, Wypall didn't, cell blew up	113	415
Paper coated with FR-C3	Electrolyte leaked @7:24 & caught fire, Wypall didn't, cell blew up	157	558
Paper coated with FR-P1	Vent popped @7:41, electrolyte and Wypall caught fire, paint charred on the can	309	N/A
Paper coated with FR-P2	Vent popped @8:06, electrolyte and Wypall caught fire, paint charred on the can	166	511
Paper coated with FR-P3	Vent popped @7:43, electorlyte and Wypall caught fire, paint charred on the can	182	507
FR painted paper	Vent popped @7:23, electorlyte caught fire, the Wypall didn't, paint charred	235	696

4.5 RETARDANT/SUPPRESSIVE COATINGS SUMMARY

EaglePicher procured four flame-retardant sprays and one flame-retardant paint to determine if they could stop propagation of fire within an aircraft battery. All flame-retardant sprays were subjected to flame and weathering tests. Three of the four sprays prevented fire. While the flame-retardant paint did not have a beneficial effect when coated directly on the cell, it performed similarly to the three sprays that prevented fire when applied to a porous substrate.

These commercial flame-retardant coatings were expected to serve as safety components external to the cell. The aircraft battery contains cell modules wrapped with a porous layer. Electrolyte and flammable gases can be ejected into the porous layer during venting or thermal runaway. The flame-retardant coatings can be coated on the fabric layer to impede fire propagation. They also could be coated on the interior of the battery case.

The three successful sprays and the flame-retardant paint were then used in cell abuse testing to examine their capabilities when exposed to an LFP 26650 cell undergoing thermal runaway. These tests involved placing a flame-retardant-coated paper towel under a 26650 cell during the overcharge abuse test in presence of a spark emitter. The control of paper towel with no flame-retardant coating caught fire when the cell was overcharged on it. The paper towel coated with the selected flame retardants did not catch fire and only showed localized charring when the LFP 26650 vented and caught fire during overcharge.

The flame-retardant paint also was tested as a coating on the cell in a similar test. The cell vented and caught fire, also igniting the paper towel. In this test, coating the cell exterior was not a valid method for controlling the spread of a flame within a battery. The same paint was then tested as a coating on a paper towel underneath an overcharged cell. The flame-retardant paint coated on the paper towel prevented flame propagation in this test.

The results of these experiments demonstrate that coating the interior porous layer with flame-retardant materials can slow the propagation of fire in a battery. FR-B was selected for coating the porous layer in later tests.

5. EMISSIONS STUDY AND SIMULATION

Effects of the two different electrolytes were investigated by determining composition of vent products formed during overdischarge or overheating, and determining pressure and temperature characteristics of 26650 cells during forced overheating. Pressure and temperature characteristics were collected on cells in open air, and also by accelerating rate calorimetry (ARC). Data was used to create an ANSYS model to simulate temperatures within a battery module during cell failure.

5.1 CELL EMISSIONS CHARACTERIZATION METHODS

Cell vent product characteristics were evaluated by measuring typical vent-opening pressure, determining thermal energy of vent products, and by analysis of vent product composition. Cell vent emissions were characterized to reveal the composition of the volatilized cell contents and demonstrate the effectiveness of the RF electrolyte. Cell venting was produced either by overcharging or overheating to initiate thermal runaway. Both of these tests result in the breakdown of electrolyte which pressurizes the cell, eventually causing ejection of volatilized material. Internal Vapor Analysis analyzed the vented gas to determine the composition.

Cell vent pressure testing was performed at room temperature on a dry cell by pressurizing with an inert gas through a drilled hole until the cell vented. An overheating test was performed on active cells by raising the temperature at 5-10°C/min to 200°C, initiating a thermal runaway, while using accelerating rate calorimetry to measure the generated heat and pressure.

Cell vent pressure, exothermic heat output, and effluent pressure measurements provide data to calculate the thermal energy of the material ejected from the vent. This information provided a starting point for future work toward safety enhancements.

5.2 CELL VENT SAMPLING RESULTS

Figure 22 shows the setup for these tests. The cell test chamber has ports and electrical feedthroughs to allow connection of the test item to a power supply for overcharging, powering a heating pad for the overheating test and for thermocouples to measure the cell and chamber temperatures. The sample tube was evacuated and sealed with Swagelok valves. The sample tube was then connected to the chamber, a pressurized inert gas cylinder and a vacuum pump through a T-junction. A cell was placed inside the chamber with the required connections for each test. The chamber and the gas sample tube were then flushed with argon and evacuated.

Figure 22. Setup for off-gas sampling test

The 26650 LFP cell was overcharged at 5A to force the cell to vent while the voltage and temperature were monitored. The off-gas was allowed inside the sample tube when the cell vented, which was then sealed by closing both Swagelok valves. Figure 23 shows the overcharge test profiles of the RF and BL cells, which were at 100% state-of-charge (SoC) at the beginning of the overcharge test. Both RF and BL cells show an increase in cell voltage. The temperature peak coincided with the sudden drop in voltage when the cell vented. Figure 24 shows the composition of the collected effluent gas, analyzed by "Internal Vapor Analysis" (IVA). The identified gas composition is similar to those reported elsewhere [3, 4].

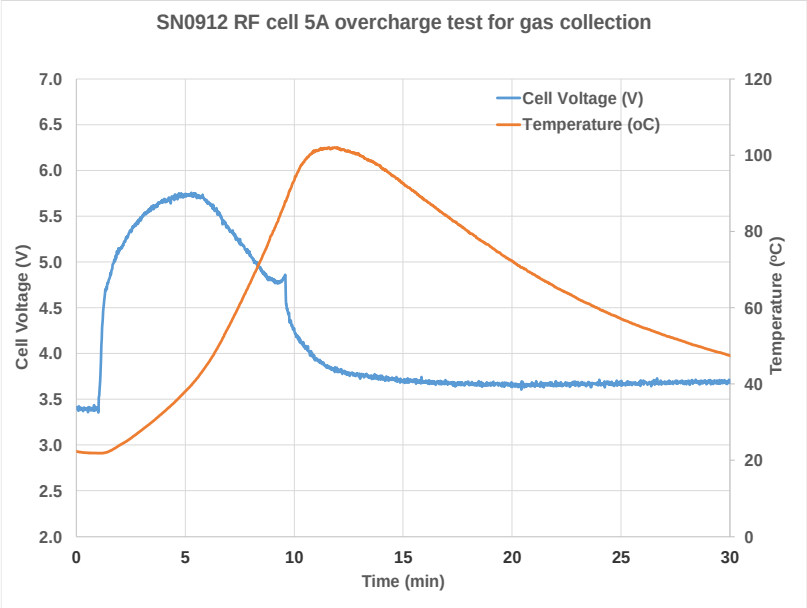

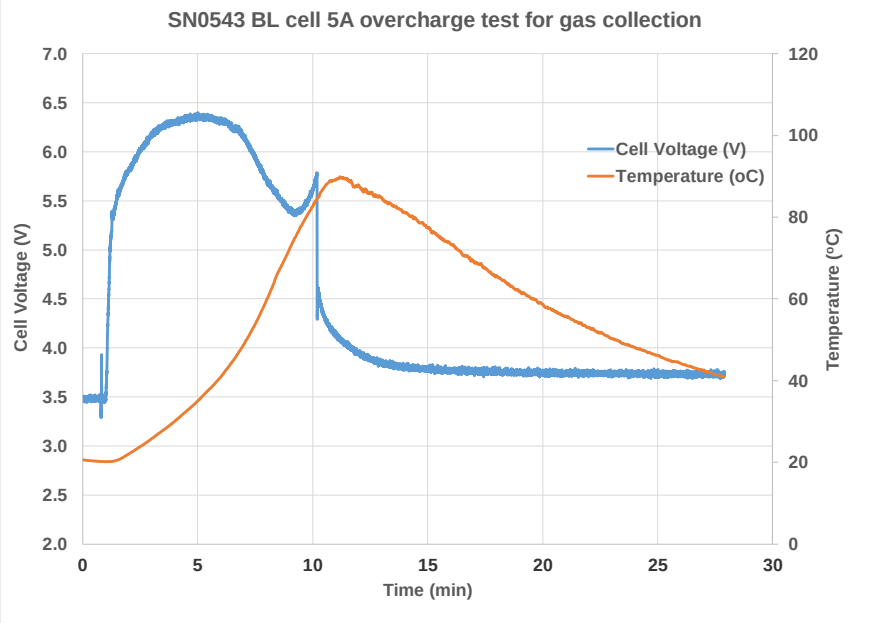

Figure 23. RF & BL cells overcharged at 5A for off-gas sampling experiment

Off-gas samples were also collected from overheating tests on separate cells at 100% SoC. The setup and procedure were the same as per prior experiment. Heating pads wrapped around the cells were used to induce the overheated state. Gas collection was done as above. The overheating test seemed to be a harsher test for these cells.

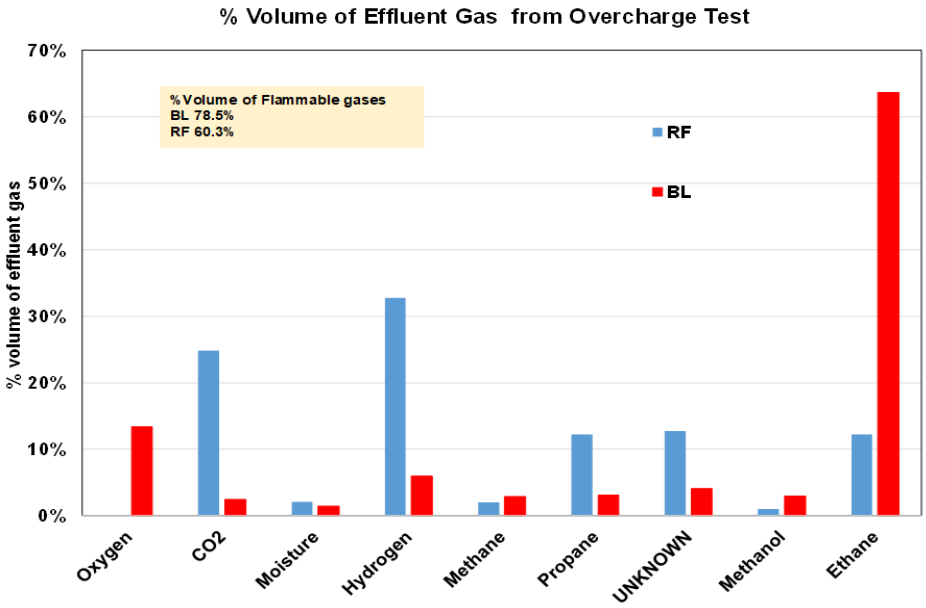

Figure 24. Effluent gas composition of overcharged cells

Figure 25 shows the effluent gas composition after the overheating test. The effluent gas from overheating contains almost twice the amount of CO_2, signifying a higher extent of combustion activity versus the overcharge test. The fraction of flammable gases, namely hydrogen, methane, and propane, was higher in the effluent from the BL cells compared to that from the RF cells in both tests.

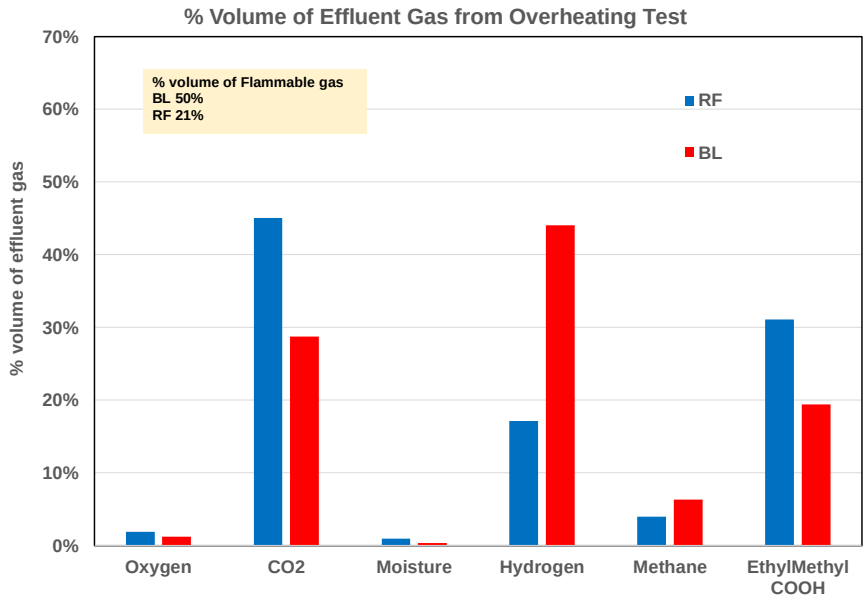

Figure 25. Effluent gas composition of overheated cells

5.3 CELL THERMAL AND MECHANICAL DATA

The cell thermal data signature was analyzed by forcing a fully charged 26650 LFP cell into thermal runaway by means of overheating the cell while measuring the generated heat and pressure using accelerated rate calorimetry (ARC). ARC tests measure thermokinetic data such as adiabatic self-heating rate, time to explosion, rate of pressure increase, maximum rate of reaction, and heat of reaction. The ARC tests were done according to ASTM Standard E1981, the Standard Guide for Assessing Thermal Stability of Materials by Method of Accelerating Rate Calorimetry.

Two types of ARC tests were performed. The first type was an open test in which the cell was heated in open air. The temperature was measured by placing a thermocouple directly on the cell. The second type was the closed test in which the cell was placed in a stainless-steel battery reservoir designed to contain test pressures below 1000 psia. The closed test also was conducted in air.

Each cell was charged to 100% SoC before starting the experiment. The cells were charged at C/2 (1.25A) to 3.65V and held there for 10 minutes. Each cell was allowed to rest for five minutes before starting the ARC test. Table 8 summarizes the results of the open tests. Each cell had multiple exotherms. Both cells showed similar weight losses of around 16%.

Table 8. Open ARC tests of RF & BL cells

Electrolyte in 26650 LFP Cell	Cell ID	Wt. Loss %	Onset T(°C)	ΔH (Cal/g)	Method
RF	A0905	16.4	131.82	33.46	Open
			186.41	>82	
BL	B1026	15.8	105.38	30.09	Open
			158.53	>94.97	

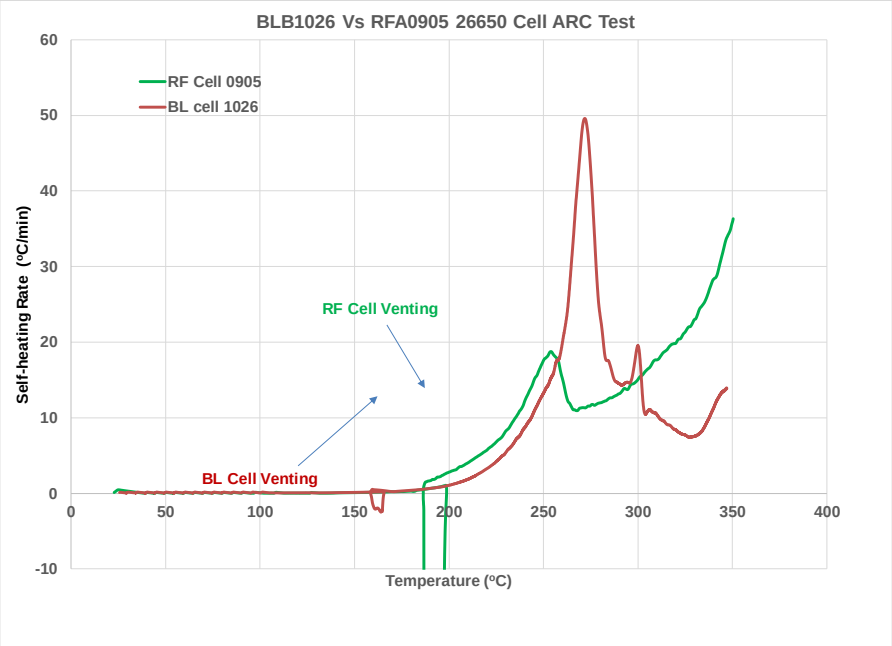

Figure 26. ARC test of 26650 cells containing RF and BL electrolytes by open-test method

Table 8 and Figure 26 show that the onset temperature of venting for the BL cell occurs much earlier at 158°C compared to the RF cell at 186°C. The 28°C higher temperature required to produce venting of the RF cell indicates lower-pressure generation rates and is an indicator for improved safety. Heat-generation measurement was facilitated by placing thermocouples directly on the cell for this experiment. Exothermic heat was calculated using the heat capacity of similar cells and the measured cell temperature. The calculated heat was 115.46 Cal/g for the RF cell and 125.06 Cal/g for the BL cell. Although the calculated heat from both cells did not show a significant difference, this is not the total heat output from the cells. The tests were stopped before the chain of exothermic reactions ended, due to the temperature limit of the testing set up (350°C). Figure 27 shows pictures of the cells at the end of the open ARC test. Decomposed electrolyte remains on the outer surface of the cell, confirming the test led to cell venting.

Figure 27. RF (left) & BL (right) cells at the end of open ARC tests, indicating cell venting

Two similar cells containing RF and BL electrolytes were tested in the closed ARC conditions, which include a stainless-steel reservoir to measure pressure. Table 9 summarizes the results of the closed ARC test.

Table 9. Closed ARC tests of RF & BL cells

Electrolyte in 26650 LFP cell	Cell ID	Wt. Loss %	Phi	Onset T(°C)	Measured T Rise (°C)	ΔH (Cal/g)	Self-Heating Rate (°C/min)	Rate of Pressure Increase (psi/min)	Max Pressure* (psig)	Method
RF	A0554	16.5	1.74	147.05	21.76	18.94	0.68	0.82	201	Closed
				174.87	148.65	129.34				
				329.76	19.9	>17.31				
BL	B0968	16.3	1.74	140.9	26.45	22.99	4.25	6.08	238	Closed
				185.05	136.97	119.04				
				333.43	16	>13.91				

*maximum measurable pressure is limited by technique

Unlike the open test, the thermocouple for the closed test was placed on the stainless-steel reservoir rather than on the cell. Although this makes it impossible to measure accurate cell temperatures in the closed method, the most important outcome is the effluent pressure measurement, which cannot be measured in the open method. The difference observed between the two electrolytes for their self-heating rate and rate of pressure increase is significant. It is 0.68°C/min and 0.82 psi/min for the RF cell, and a much higher 4.25°C/min and 6.08 psi/min for the BL cell. Figure 28 and Figure 29 show the RF and BL self-heating and pressure-increase data.

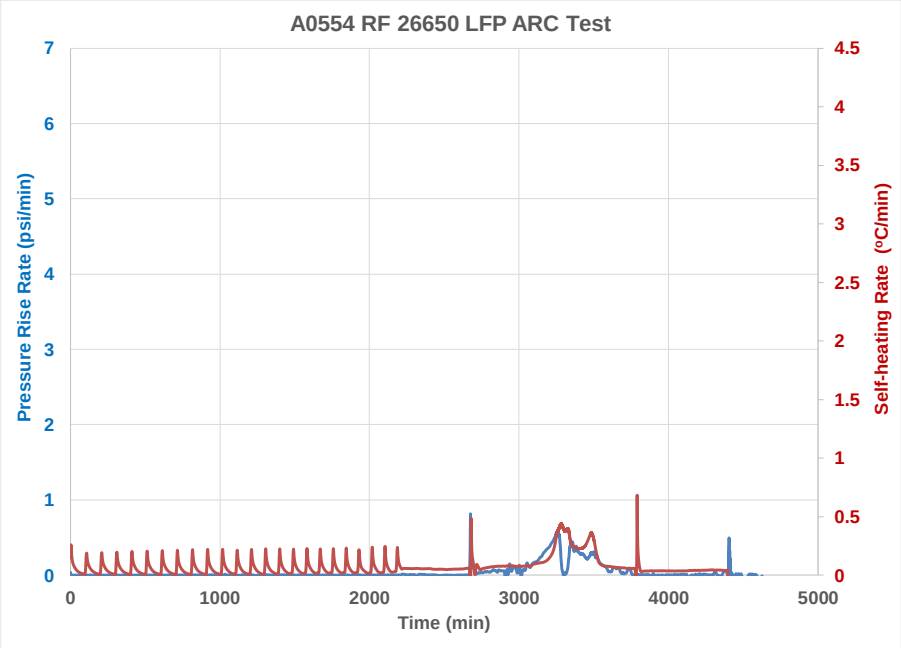

Figure 28. Pressure-rise & self-heating rates of RF electrolyte cell in the ARC test

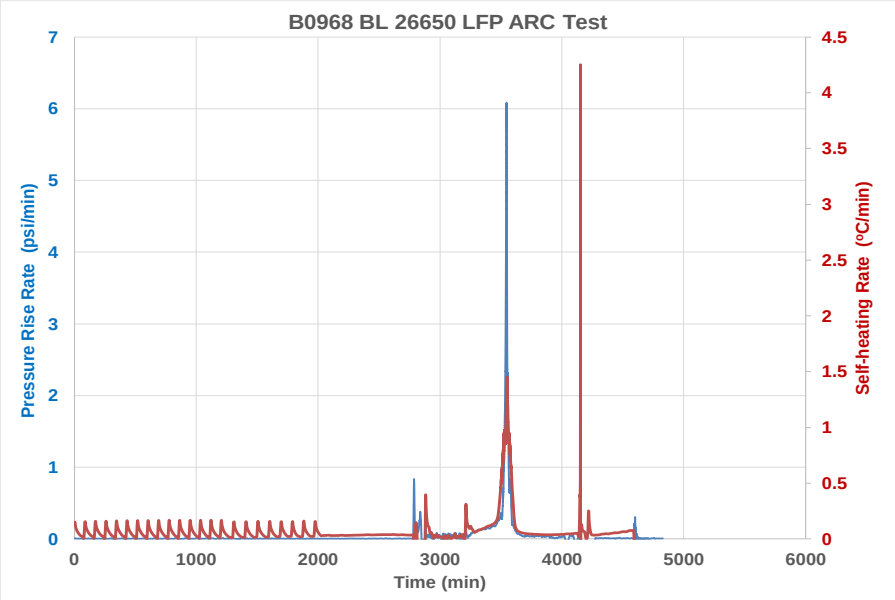

Figure 29. Pressure rise & self-heating rates of BL electrolyte cell in the ARC test

The higher onset temperature for the exothermic reaction combined with the slower rate of increase in both temperature and pressure reinforces the safer performance shown by the RF cells in the abuse tests. The BL cells produced more incidents of fire in the abuse tests, which can be explained by their demonstrated higher rate of pressure buildup. The measured pressure also was lower for the RF (200 psig) compared to the BL cell (238 psig). However, these values do not reflect the overall pressure generated by the cells because the experiment was stopped at 350°C due to the thermal instability of the O-rings used in the reservoir.

Figure 30 shows pictures of BL and RF cells at the end of the closed test. The closed test shows more cell vent products than in the open tests, likely due to the placement of the cell in a hermetic reservoir to hold the pressure until the endpoint of 350°C.

Figure 30. RF (right) and BL (left) cells at the end of closed ARC tests, showing profuse cell venting

To understand the response of a battery in an abuse test, the cell's energy under abusive conditions must be measured to evaluate the cell's mechanical design in terms of pressure containment before safe release. ARC tests led to the measurement of heat of the exothermic reactions and the accompanied pressure generation from the cells under abusive conditions. Additional experiments were carried out to check the cell mechanical features, such as cell vent pressure.

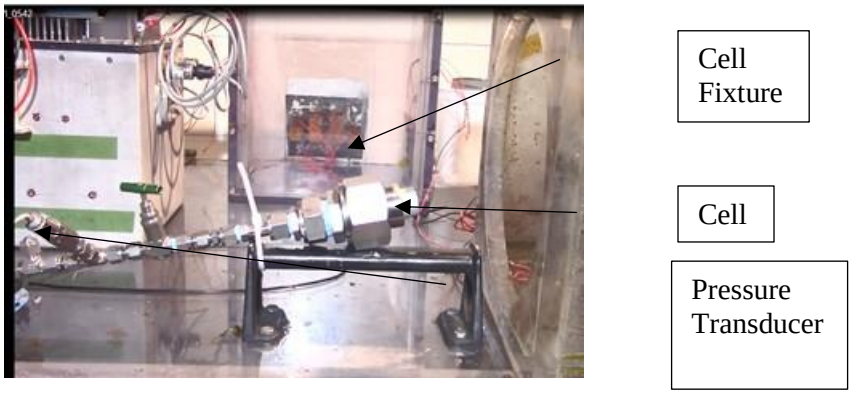

Figure 31. Experimental setup to measure cell vent pressure

Figure 31 shows the experimental setup for the vent pressure measurement. A pressure transducer was placed in-line to measure the pressure as a function of time. The cell was pressurized by passing the inert gas through two holes drilled in the header. The cell was secured in the fixture with epoxy. This experiment was designed to evaluate the maximum pressure that the cell can withstand before venting. The average vent pressure for two cells was 400 psi. Figure 32 shows the pressure-versus-time plot and a picture of the cell at the end of the test. The picture shows the vent ruptured, and the jelly roll was expelled at the end of the test.

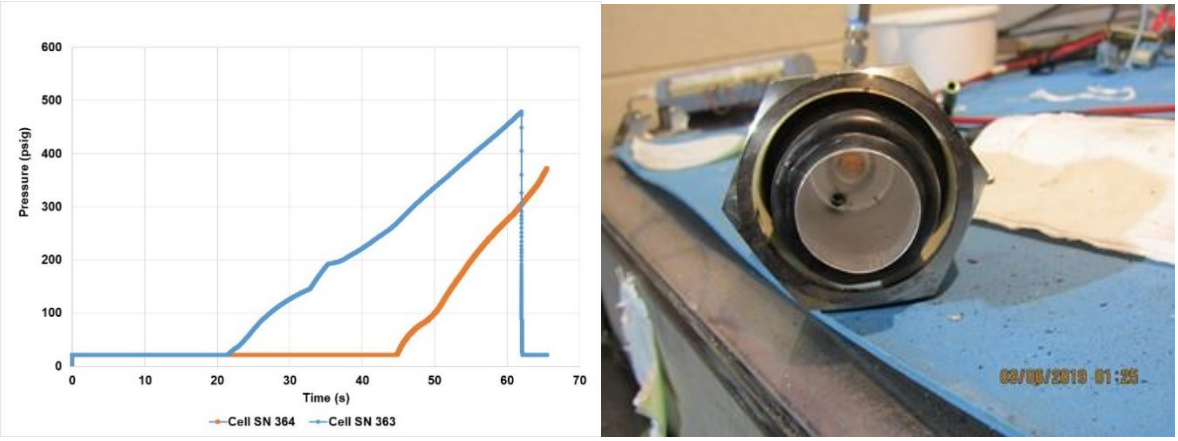

Figure 32. Vent pressure plot & cell appearance at end of test

The actual pressure generated by a cell during a real-time thermal runaway was measured in the overheating test. These tests were performed in the same fixture that was used in the off-gas sampling experiment; a hermetic test fixture with a free volume of 36 in^3 (590 cc), shown in Figure 22. A pressure transducer was connected in-line instead of the gas sampling tube.

Overheating tests were performed on active 26650 LFP cells. Figure 33 shows the single cell overheating test. The maximum-measured chamber pressure was 48 psig and the maximum cell temperature was 355°C. Figure 34 shows the test with two cells connected in parallel. The maximum measured pressure was 83 psig.

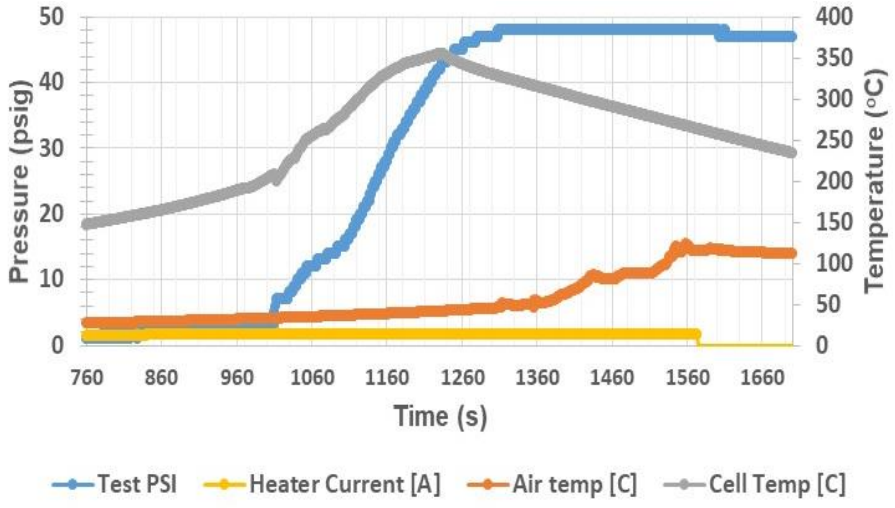

Figure 33. Single-cell overheating to measure pressure generation

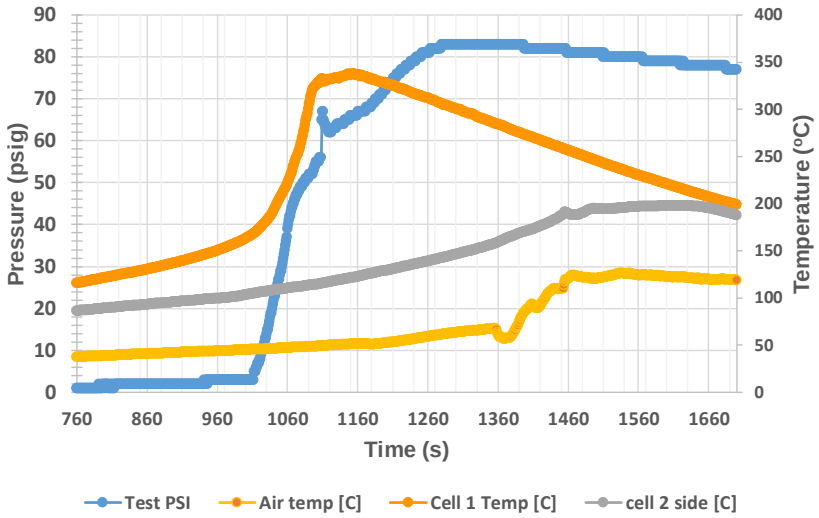

Figure 34. Two-cell overheating to measure pressure generation

5.4 THERMAL ENERGY TRANSFER MODELING

The EaglePicher aircraft battery contains 26650 LFP cells in the configuration of 21P8S. However, for this effort, we chose a reduced 7P2S battery module configuration (additional information on the module design can be found in Section 6. to assess the contrast between the BL and RF version in the abuse tests. The 7P2S configuration represents a simplified means to repeat the test for different needs while preserving the cell grouping and layout used in the full-sized aircraft battery. The module sleeve, ceramic fabric wrap, divider, case material, and vent, are made of the same materials used in the current aircraft battery. The amount of free space is proportional to the full aircraft battery.

It was possible to measure the cell heat output, off-gas composition, and the pressure generation for both BL and RF chemistries using the off-gas analysis, ARC test, and pressure measurements. ANSYS simulation was performed on a CAD model of the module to extrapolate the cell level thermomechanical parameters to the module level. Figure 35 shows the CAD model of the representative battery assembly. It consists of two 7P modules connected in series and separated by a divider. Each submodule consists of seven cells in parallel, a Lexan enclosure, and electrical connection plates. The thermal model was created by applying a heat flow to each cell, equivalent to the measured values from the ARC tests.

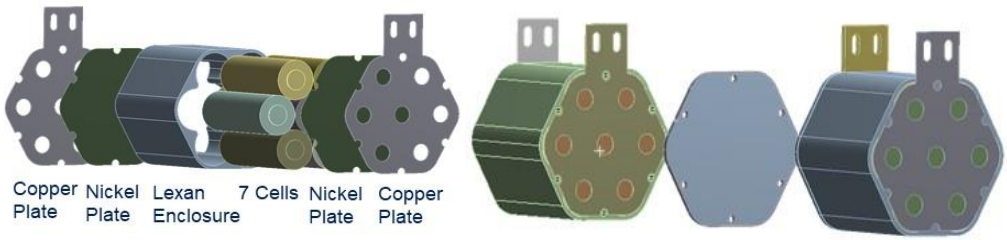

Figure 35. Images of 7P submodule (left) and 7P2S module (right) used for thermal modeling

The overcharge test condition was chosen for modeling. The measured heat, pressure, self-heating rate and rate of pressure increase from the ARC measurements were incorporated into the ANSYS thermal model of the baseline assembly. Figure 36 shows the temperature distribution used at the beginning and end of the simulation.

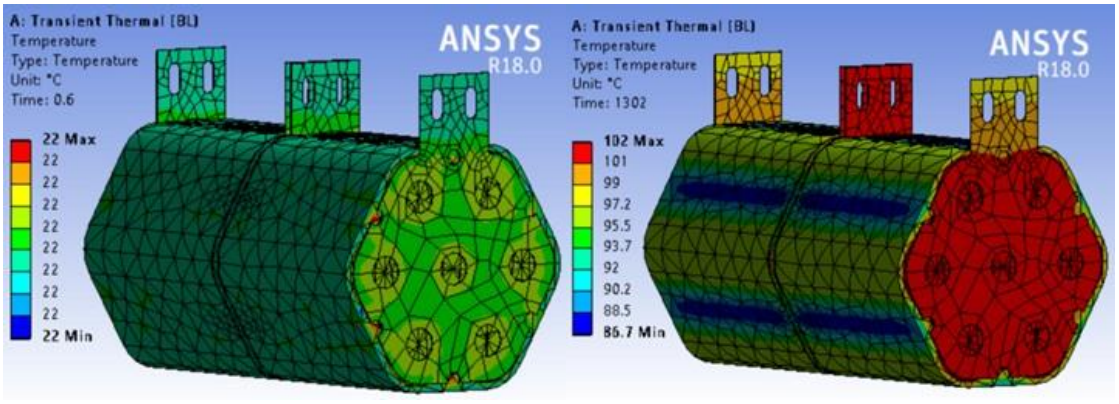

Figure 36. Thermal modeling of BL assembly in overcharge testing at beginning (left) and end (right) of overcharge

Figure 36 also shows it took 1,302 seconds (21.7 minutes) for the battery to reach a maximum temperature of 102°C, at which point the BL cells will vent. However, this model does not account for the heat generation and ignition of off-gases by a spark emitter, which is incorporated for the module abuse testing. Figure 37 shows the thermal modeling of the RF battery assembly.

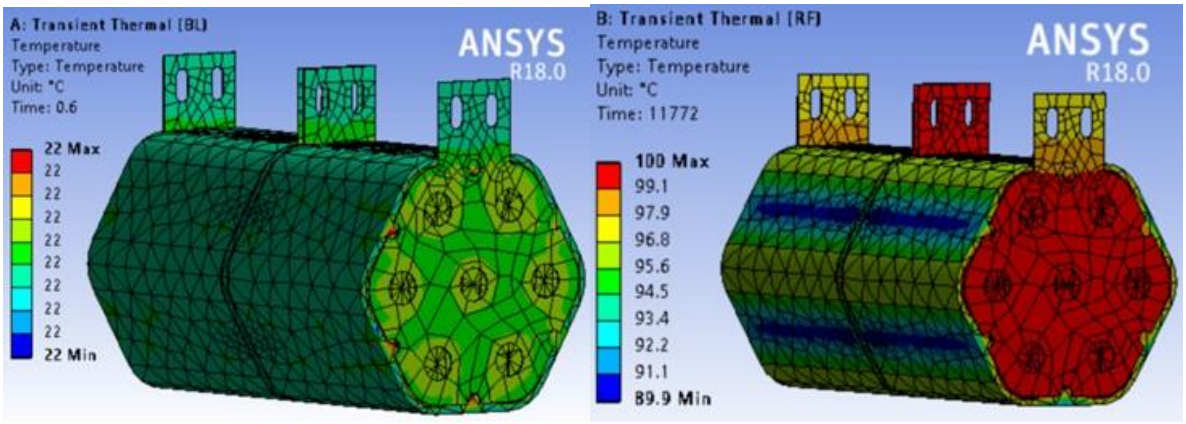

Figure 37. Thermal modeling of RF assembly in the beginning (left) and end (right) of overcharge test

It takes 196.2 minutes to reach a maximum temperature of 100°C across all cells in the RF module. This thermal model shows the heat generation and the time for propagation in BL and RF cells in the overcharge tests without secondary devices such as a spark emitter. The increase in the time taken to reach the venting temperature is an important factor for increasing the safety of a battery. Faster heat generation leads to a rapid increase in pressure, resulting in a more violent reaction to abusive conditions.

5.5 EMISSIONS AND SIMULATION SUMMARY

Vent characteristics of cells with both RF and BL electrolytes were evaluated by off-gas analysis, ARC, and vent testing to measure the self-heating rate, pressure-rise rate, heat output and cell vent pressure. The measured parameters were incorporated in a thermal model to simulate the responses of RF and BL battery modules in an overcharge test. The off-gas analyses were performed on effluents from both RF and BL cells, resulting from both overcharge and overheating tests. Effluents from RF cells contained a lower percentage of flammable gases, such as hydrogen, methane, and propane in both tests. This supports the observed safer response of RF cells in the single cell abuse tests. The overheating test was found to be more abusive to the cells than the overcharge test as measured by the higher percentage of CO_2 in the effluent gas, indicating a higher degree of combustion during thermal runaway.

The RF and BL cells showed similar amounts of heat generated from exothermic reactions in ARC testing. However, the rates of heat and pressure generation were much lower for the RF cells, at 0.68°C/min and 0.82 psi/min compared to 4.25°C/min and 6.08 psi/min for the BL cells. This again supports the outcome from the single cell abuse tests. The RF cell also demonstrated a higher onset temperature of the decomposition reaction of 132°C compared to the BL cell (105°C). The earlier onset of the decomposition reaction combined with the higher rates of temperature and pressure increase in BL cells is consistent with their higher incidences of thermal runaway in the single cell abuse tests. Table 10 summarizes the results from these analyses.

Table 10. Summary of emission characterization tests

Electrolyte in 26650 LFP Cell	ARC Test					Gas Analysis	
	Onset T(°C)	ΔH (Cal/g)	Self-heating Rate (°C/min)	Rate of Pressure Increase (psi/min)	Max Pressure (psig)	% Flammable gas from Overcharge	% Flammable gas from Overheating
RF	131.82	33.46	0.68	0.82	201	60.3	21
	186.41	>82					
BL	105.38	30.09	4.25	6.08	238	78.5	50
	158.53	>94.97					

The cell vent test was conducted on dry cells by drilling holes in the cell header and pressurizing with inert gas. The vent disc failed at 400 psi.

In a normal cell containing electrolyte, venting can happen due to pressure buildup from the vapor and gas generation in the cell. Therefore, the pressure generation from a real cell was measured by subjecting single and paired baseline cells to overheating tests. The single cell overheating test resulted in a generated pressure of 48 psig and skin temperature of 355°C. The cell vented in both cases through the ball seal and/or the vent disc.

Finally, a thermal model was made for both RF and BL modules using ANSYS software. All components of the module were included in the modeling. The heat and rate of pressure increase from the ARC measurements were used for the simulation. The overcharge test was chosen as it can lead to a more uniform failure in the module. The ANSYS model shows that the main

difference in the response of the two chemistries is the time for the temperature to rise and cause venting, which was 21.7 minutes for the BL module and 196.2 minutes for the RF module. Slow heat and pressure generation in the RF module are very important in achieving a less volatile response in abuse tests.

Based on the thermal modeling, the RF module shows a higher margin of safety. The response time of the module in the actual testing may be shorter than the simulated results since no spark emitter was included in the ANSYS model. The time difference between the BL and RF venting may still be realized, however, in the real module-level testing.

6. PROTOTYPE MANUFACTURING

The final step in understanding the overall effect of the multiple Li-ion failure mitigation technologies described above requires integrating all improvements into a representative battery module and comparing its response to thermal runaway events outlined in DO-311A to a control battery without those improvements. The test assembly chosen to evaluate the improvements was based on an existing EaglePicher aircraft battery designated as MAR-9653, and which is composed of 168 26650 Li-ion cells in a 21P8S arrangement. Due to project constraints, the integration test unit was scaled down to a 7P2S arrangement, but which otherwise was assembled using the same techniques as the full-sized MAR-9653 battery. The sub-scale prototype assembly included all other supporting design methods, mitigations, and functional elements necessary to support qualification through DO-311A and DO-160G, including battery case, vent, cell insulation/ isolation, etc. However, continuing through a full TSO certification was beyond the scope of this project. The battery management system was omitted from this design and build effort. The impact of the electronics is discussed relative to their integration into the battery. This section addresses the sub-scale battery design, manufacturing methods, performance testing data of subsystems, integration plan, testing criteria, and validation plan.

6.1 MANUFACTURING METHODS & ISSUES

The EaglePicher aircraft battery assembly, MAR-9653, is constructed with a 21P8S cellblock utilizing commercial 26650 LFP cells. A smaller representative battery was developed for this project that provided the same cell failure mechanisms and propagation behavior as the current EaglePicher aircraft battery design.

As noted in Section 5. , the smaller prototype battery assembly designed for this project consists of 26650 LFP cells arranged in a 7P2S configuration. This smaller battery size preserved the negative-to-positive cell layout between sections, as well as the adjacent cell placement utilized within the MAR-9563. For clarification in this section, each 7-cell section is termed a battery submodule. The assembly of two 7-cell sections into the full 7P2S unit is termed a battery module.

The constituent parts used for this project are the same materials and construction utilized for the MAR-9563 battery. The prototype battery includes additional thermocouples and a pressure transducer for the planned testing, as well as ports for electrical power and heater interfaces needed to cause cell failure. It also includes a spark emitter to aggravate failure mechanisms and help demonstrate the benefit of the new safety technologies, though DO-311A does not require the inclusion of a spark emitter for the cell failure tests. As they were not part of this project, the

electronic design elements were not incorporated into the design implementation of the prototype test battery.

Figure 38 shows the cell submodule sleeve that constrained the seven cells. The sleeve was machined from a solid block of Lexan 3412R to yield a slight interference fit for the cells, intended to eliminate the need for adhesives.

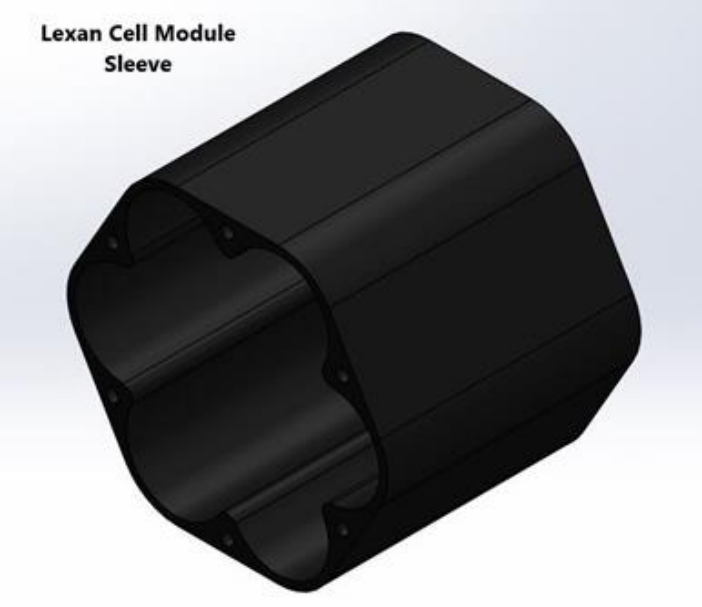

Figure 38. Cell submodule sleeve

Figure 39 shows 0.005” thick nickel bus plates that were ultrasonically welded to the 0.015” thick copper bus plate. Interconnecting cell bus plates were used to couple the individual cells within the submodule. The bus bars serve as the external electrical connections for the finished test battery assembly. These current carrying materials were designed according to their expected load and tolerable thermal rise:

Bus plate ampacity (steady state):

- 30°C rise – 187A
- 50°C rise – 250A
- 65°C rise – 285A

Bus bar ampacity (steady state):

- 30°C rise – 270A
- 50°C rise – 360A
- 65°C rise – 415A

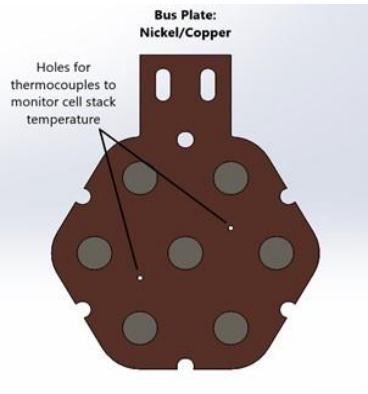

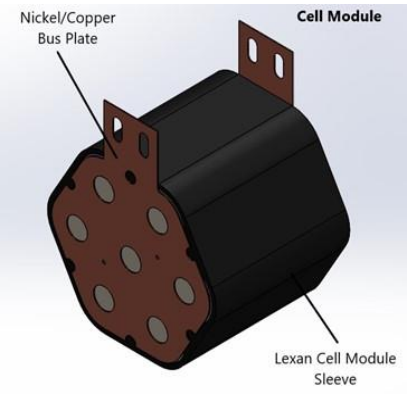

Figure 39. Bus Plate **Figure 40. Single 7p Cell submodule of test battery**

Figure 40 shows the final 7P submodule after the bus plates were welded with six spot welds per cell to attach a bus plate to each end of the cells in the Lexan sleeve.

Figure 41 shows the placement of the two 7P submodules with a single Lexan divider. Figure 42 shows the two submodules fastened together by two stainless steel screws. The bus plates were connected to the bus bar by stainless steel screws. Four AWG power cables were then attached to the bus bars. Five thermocouples were utilized to record the temperature at different battery locations. Two thermocouples monitored the temperature of the center cell on each submodule, and the fifth thermocouple was used to measure the internal temperature near the battery vent (not shown).

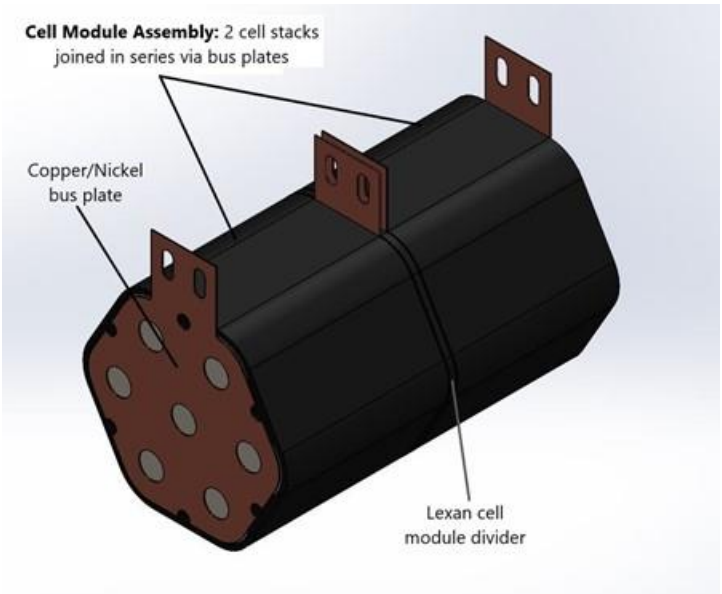

Figure 41. Cell module assembly

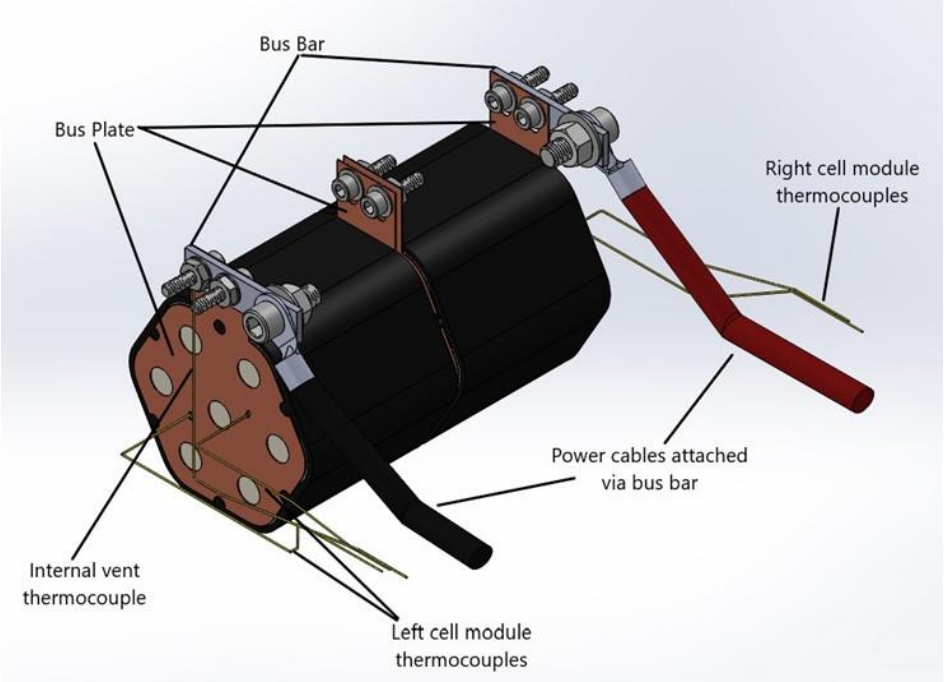

Figure 42. Fully connected test module battery

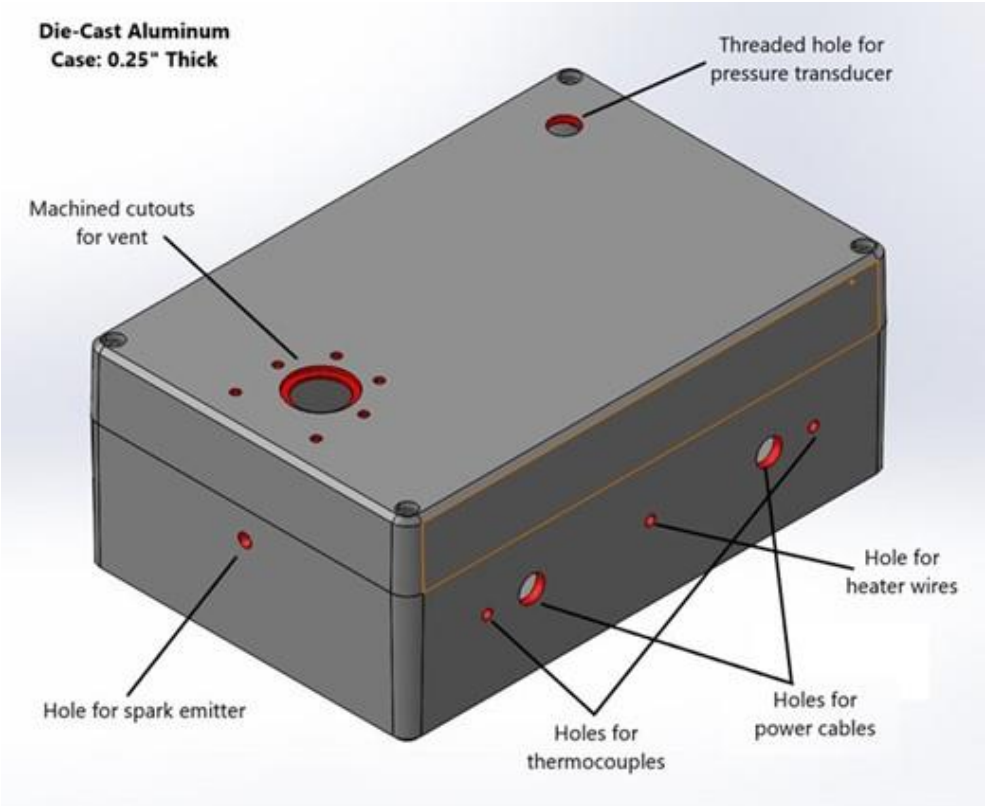

Figure 43. Battery assembly case design

Figure 43 shows the battery assembly case. It was constructed from die cast aluminum with ¼-inch-thick walls. The case has machined cutouts for the external vent mechanism and the pressure transducer on top of the case. The case also has cutouts machined for the installation of a spark emitter on both ends. Two ports for thermocouples and power cables are also included. Additional ports are included for the heater wires for the overheating test. Figure 44 shows the finished test unit located in the aluminum container. The fire-retardant material is wrapped around the two cell submodules (not shown). The supporting electronics normally present in a Li-ion aircraft battery are not included in this test item as noted elsewhere. However, the aluminum battery assembly case was sized such that the free void volume within the container is the same as a fully configured aircraft battery.

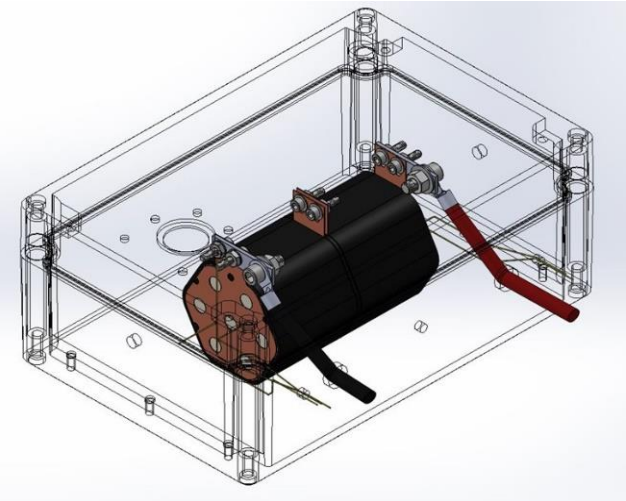

Figure 44. Assembled test battery

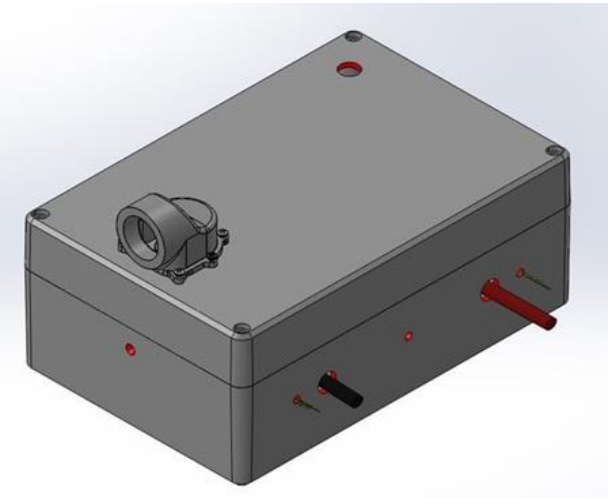

Figure 45. Final test battery assembly

The test unit also included a custom vent mechanism that supports the expected volume of cell emissions and addresses the need for internal isolation from moisture during normal battery use. Figure 45 shows the battery assembly with this vent mechanism shown as a port on the top side.

This battery design served as the basis for the various safety tests comparing the improvements of this project and the original baseline. It either includes all of the safety technologies discussed in this report or none, i.e., an "all or nothing" comparison. The 26650s for the "all" case contained the RF electrolyte. The interior wall surface of the case was manually coated with the flame-retardant paint, and the porous cell wrap material was sprayed with the flame-retardant spray. The "nothing" case used cells with the BL electrolyte and did not include either of the flame-retardant materials.

6.2 PERFORMANCE TESTING DATA OF SUB-SYSTEMS

Performance comparisons of RF and BL containing batteries were conducted per the guidelines from DO-311A. The FAA allowed the electrical performance tests at the cell level since the module does not contain a battery management system (BMS).

Cells selected for the submodule had a similar open-circuit voltage (between 3.28 and 3.30 V) and discharge capacity at C/20 (2.6 to 2.75 Ah). Cells also were tested at higher discharge rates at room

temperature. Figure 46 shows the discharge capacity and temperature response for these tests. The temperature profiles of the RF and BL cells are similar, indicating no unusual impedance increase with the RF electrolyte during discharge at high rates (1C to 12C or 2.5A to 30A). At the 12C rate, the RF cell showed a sloped plateau and a lower capacity than the BL cells. However, the performance was the same for both electrolytes at the 8C discharge rate required for MAR-9563.

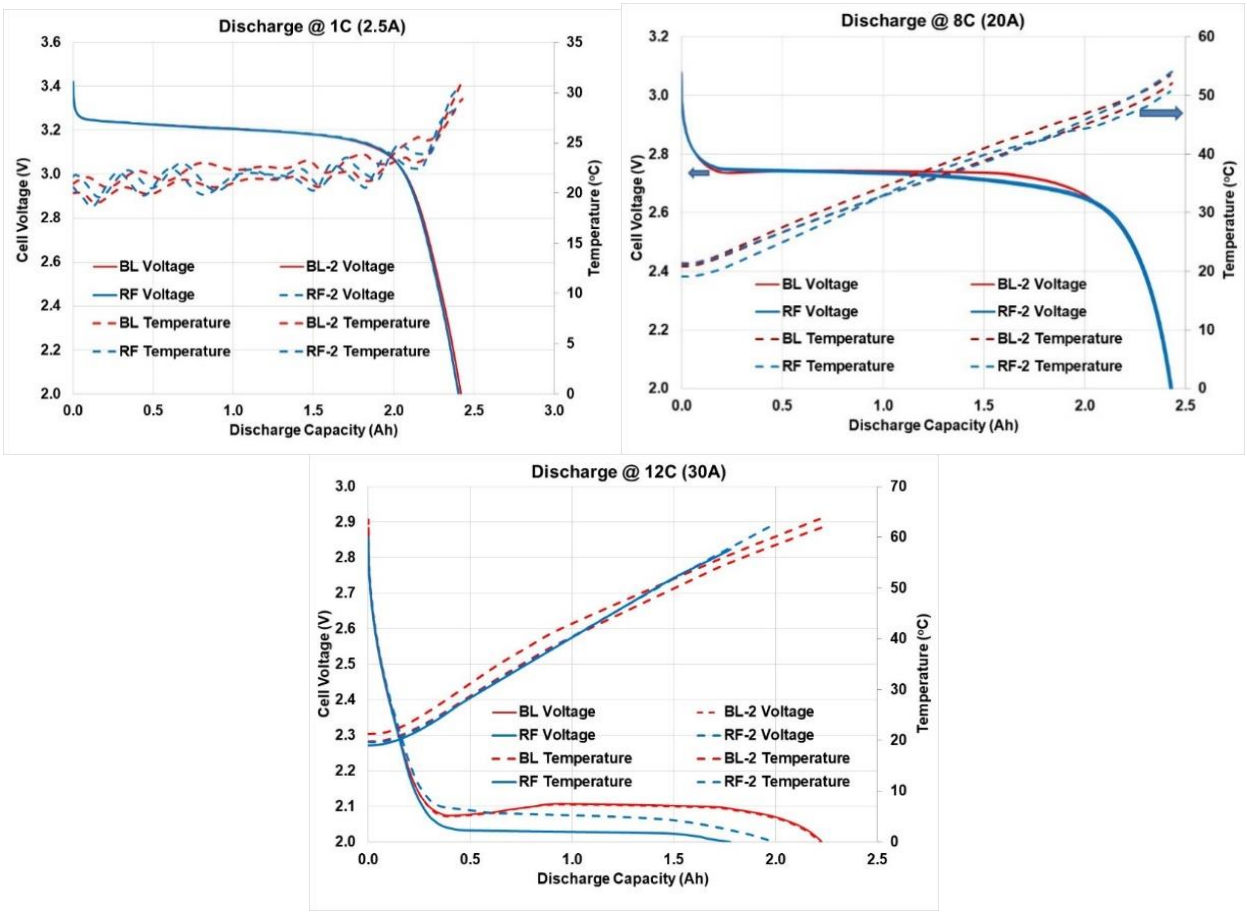

Figure 46. Discharge capacity and temperature response at 1C, 8C & 12C rates

Figure 47 shows the cycling of both RF and BL cells when charged at a C/5 rate and discharged at a 1C rate. Cells with both electrolytes demonstrated similar capacity retention after 300 cycles. A slight improvement of performance by RF at early cycles was offset by a slight decrease in performance at the later cycles.

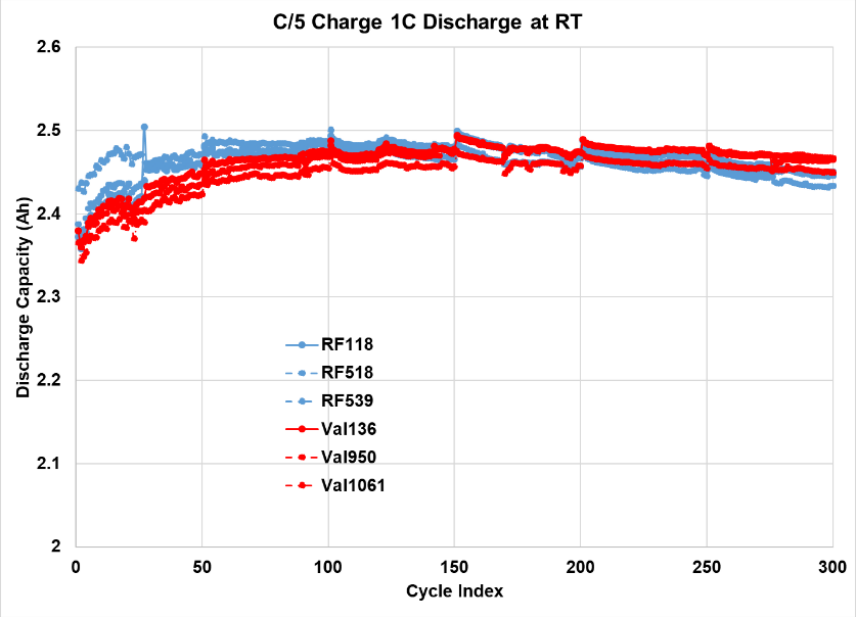

Figure 47. Cell charge/discharge cycling response at 300 cycles

These tests show similar electrical performance between the RF and BL cells, necessary for a fair comparison of the failure tests.

6.3 INTEGRATION PLAN AND TESTING CRITERIA

Table 11 shows the electrical performance tests. Both RF and BL cells were evaluated simultaneously to avoid environmental or test equipment variation. At least two cells of each kind were subjected to the electrical tests.

Table 11. Planned cell-level electrical tests

DO-311A Reference No.	Performance Test Description
2.4.4.5	Capacity Test (at +23°C)
2.4.4.6	Capacity Test at Low and High Temperatures (-20°C, and +50°C)
2.4.4.8	Charge Acceptance Test
2.4.4.10	Cycle Test for High Rate Batteries

The outcome of these performance tests was used solely for comparison and contrast of the two electrolytes; no absolute criteria was applied to gauge acceptability of the outcome.

Failure testing was performed on the batteries built as described above. Based on the response of the BL battery to the three individual abuse tests, the most critical tests were selected to run on the improved battery that incorporates the RF electrolyte and coating mitigations. The response of the improved battery was then compared and contrasted to the BL battery behavior.

Table 12. Planned battery-level failure tests

DO-311A Reference No.	Failure Test description
2.4.5.2	Short Circuit Test of a Battery without Protection
2.4.5.5.1	Test Method for Battery Thermal Runaway via Overcharging
2.4.5.5.2	Test Method for Battery Thermal Runaway via Overheating

The outcome of these failure tests was used for comparison and contrast of the improved battery to the BL assembly. The goal was compliance to Section 2.2.2.1 for Short Circuit, and Section 2.2.2.4 of DO-311A.

6.4 PRODUCT READINESS REVIEW DATA

A scale-up plan was necessary to address the potential impacts of integrating the new safety approaches.

- Cell stack—Although the EaglePicher aircraft battery utilizes a larger cell stack than the test battery design outlined above (21P8S vs. 7P2S cell stack), the cell sizes are identical. Since the cells incorporating RF electrolyte had demonstrated comparable performance to the BL version, new RF cells could simply replace those within the existing 21P8S cell stack with the same restraints and interfaces.
- Battery electronics—As the RF cell utilizes the same electrochemistry as the BL, and with the demonstrated comparable performance, no BMS calibration changes would be necessary to address charge control or out-of-bounds fault limits utilized to enact the existing overcharge, overdischarge, overtemperature, undertemperature, or overcurrent protection limits. The BMS and battery electronics subsystems would therefore remain unchanged.
- Fire-retardant coatings—Inclusion of the flame-retardant paint for the internal surfaces of the battery case and the spray coating to be applied to the existing porous material surrounding the cell stack did not result in an appreciable increase in thickness of the battery components. Coating processes readily available in-house would be applicable to replace the manual coating utilized for this project.
- Cell vent mechanism—The same design presently utilized within the EaglePicher aircraft battery assembly was utilized within the test batteries outlined earlier and demonstrated suitable behavior to manage cell emissions during a failure condition. No changes would be required.
- Battery case—Although the test battery was a reduced design, it uses an aluminum enclosure comparable to that formed for the aircraft battery. Cell failure testing indicated no need for change to address thermal response behaviors. No changes to the existing battery case would be required.
- Other battery content—All other components are otherwise unchanged as the included safety technologies enable a seamless integration into the present MAR-9563 battery design.

Note that the present MAR-9563 aircraft battery consists of 26650 LFP cells. The original intent of this project was to develop NCM-based cylindrical cells utilizing the RF electrolyte. However, the NCM 18650 was dropped from further study due to the relatively low discharge-rate capability. Cell testing continued but with the LFP 26650 cell. If a suitable 18650 NCM cell candidate becomes available, the resulting cell stack will be notably different due to the increased energy and reduced size. Such a cell would only require 7 series-connected groups of cells vs. the present 8 and, depending upon the resulting capacity and discharge-rate capabilities, a smaller volume of parallel-grouped cells. A change in electrochemistry from LFP to NCM would also require commensurate changes to the BMS, a redesign of the cell interface locations, and a smaller overall battery case.

7. BATTERY SYSTEM TEST AND VERIFICATION

The representative aircraft battery that was described above was evaluated in accordance with DO-311A to more completely compare the safety improvements of the reduced flammability design with the baseline. Testing methods for cell-level electrical tests and battery-abuse tests were outlined in Table 11 and Table 12.

7.1 SYSTEM PERFORMANCE ELECTRICAL TEST RESULTS

7.1.1 Capacity Test at 23°C (2.4.4.5 of DO-311A)

The rated capacity of the 26650 LFP cell is 2.5 Ah at the selected I_{max} rate of 0.2C. Figure 48 shows cells containing both electrolytes delivered full-rated capacity at I_{max}. The average energy was 7.46 Wh for both cells.

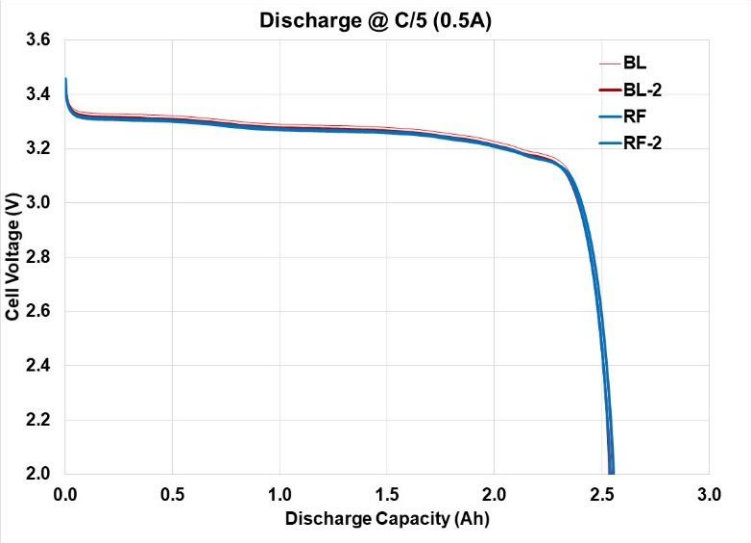

Figure 48. Capacity test @ 23°C

7.1.2 Capacity Test at Low and High Temperatures (2.4.4.6 of DO-311A)

A cell-level test at −20°C was used to demonstrate the low-temperature capability of the RF cell as a heater is used in the MAR-9563 for low temperature. However, both cell chemistries were tested between −30°C and 50°C to demonstrate the electrolyte effect on temperature capability. At

−30°C, both RF and BL cells were charged and discharged at the C/20 rate. RF cells showed a higher capacity than BL cells at this rate and temperature. Cells were tested at a 1C discharge from −20 to 50°C. Figure 50Figure 50 shows the 1C rate discharge energy was similar at all tested temperatures.

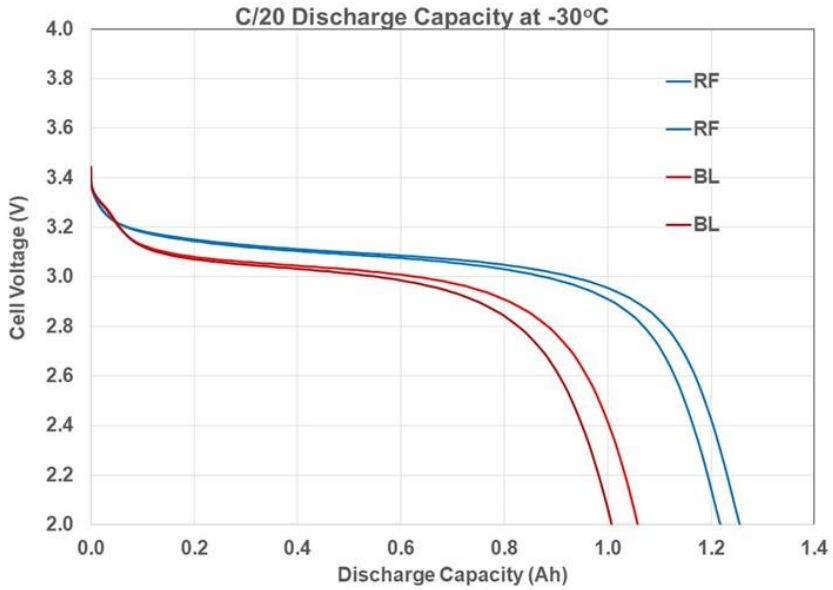

Figure 49. Discharge profiles of LFP 26650 cells at -30°C and C/20 rate

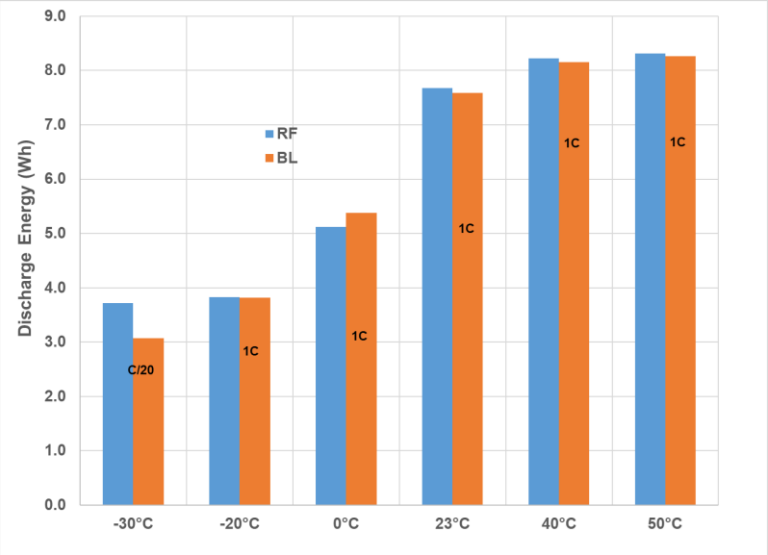

Figure 50. Discharge energy at 1C rate over a wide temperature range

7.1.3 Charge Acceptance Test (2.4.4.6 of DO-311A)

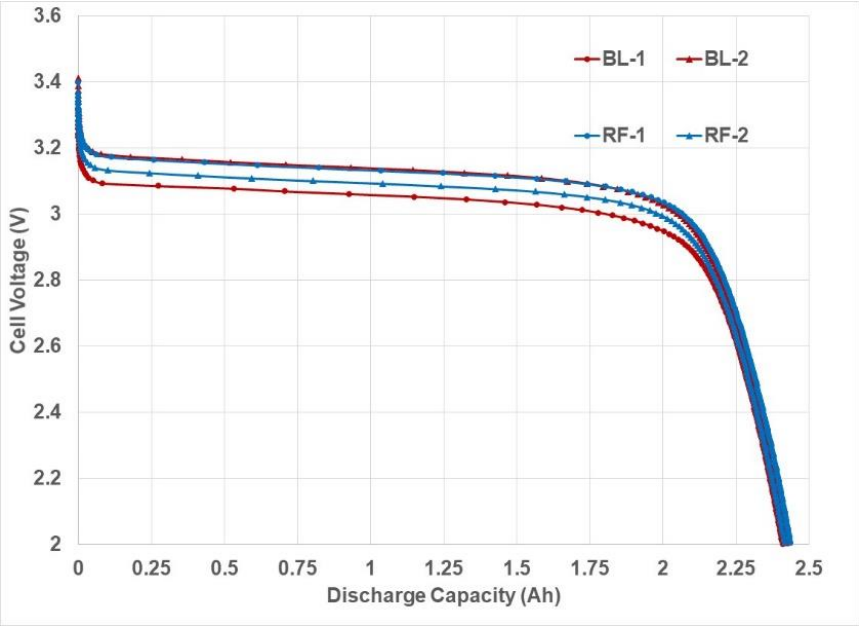

Figure 51. Charge acceptance test at 1C rate

The cells were charged and discharged at 1C rate per DO-311A, paragraph 2.4.4.8.1. Both RF and BL cells delivered similar capacity for charge and discharge. The RF and BL cells accepted 2.6Ah during charge at the 1C rate and delivered 2.4Ah when immediately discharged at the 1C rate. It is typical for Li-ion batteries to have about 10% higher-charge capacity than discharge capacity due to the documented, irreversible capacity loss in the anodes; they cannot be 100% delithiated during discharge [6].

7.1.4 Cycle Test for High-Rate Batteries (Paragraph 2.4.4.610 of DO-311A)

RF and BL cells were cycled at the manufacturer-recommended rate of charge (C/3) for one hour, followed by a 4C discharge to 20% depth of discharge (10A discharge for 3 minutes). This was repeated for 100 cycles with a one-hour rest between discharge and charge steps. The cells were then charged and discharged at a 1C rate to measure their capacity. This capacity check (Paragraph 2.4.4.5 of DO-311A) was performed to measure actual capacity against the rated capacity. Both RF and BL cells delivered 94% of rated capacity after this test. They did not show any increase in impedance or heat, as shown by the constant discharge capacity in Figure 52. The maximum measured skin temperature was 24.5±0.4 °C for both types of electrolyte. Therefore, the RF battery is expected to perform similar to the BL in a battery-level electrical test.

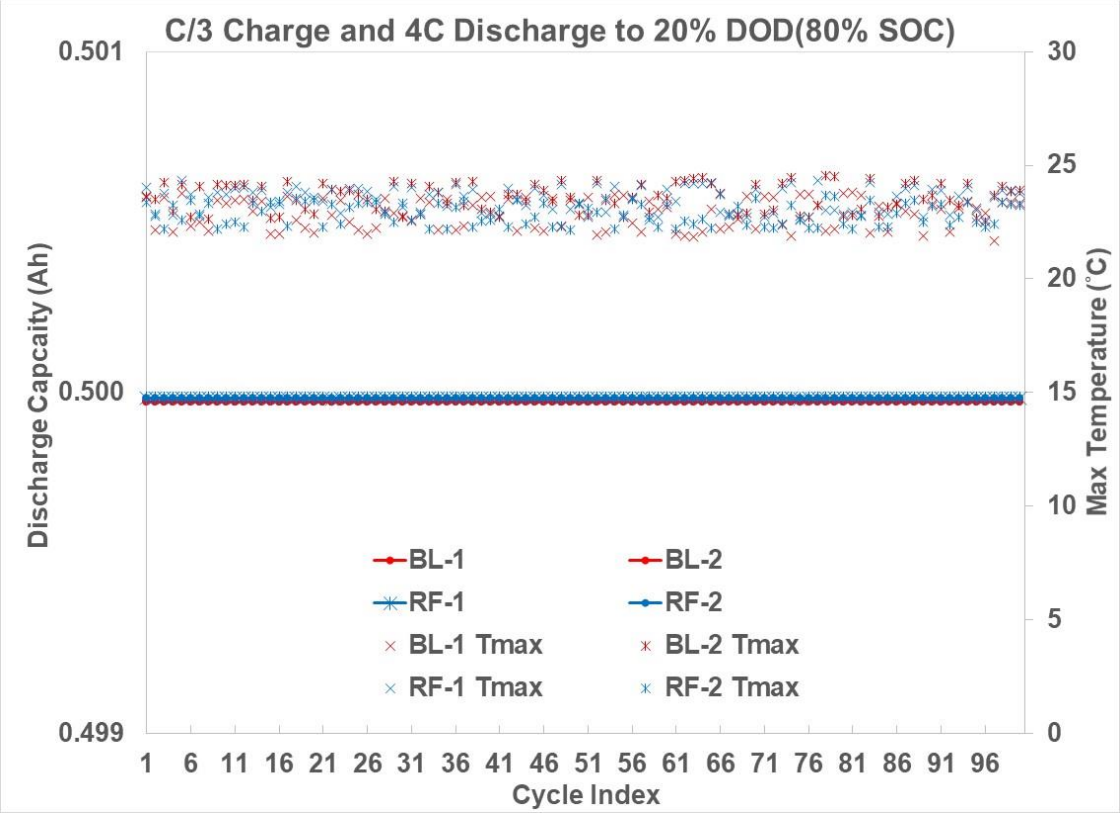

Figure 52. High-rate cycle test of 26650 LFP cells at 23°C

Table 13 summarizes the effect of 100 high rate cycles on the stability of RF and BL cells. The cells demonstrated 95% of the rated capacity after 100 cycles at the 1C rate. They also showed 94% efficiency for the charge acceptance test later. This shows cells with RF electrolyte perform similar to BL with no apparent degradation from the high-rate cycling test.

Table 13. Effect of high-rate cycling on 1C discharge capacity

Electrolyte	C1	C2	%C1	%C2
BL	2.38	2.36	95%	94%
BL	2.39	2.36	96%	94%
RF	2.38	2.36	95%	94%
RF	2.38	2.36	95%	94%

7.2 SYSTEM PERFORMANCE ABUSE TEST RESULTS

7.2.1 Baseline Battery Overcharge Test (Paragraph 2.4.5.5.1 of DO-311A)

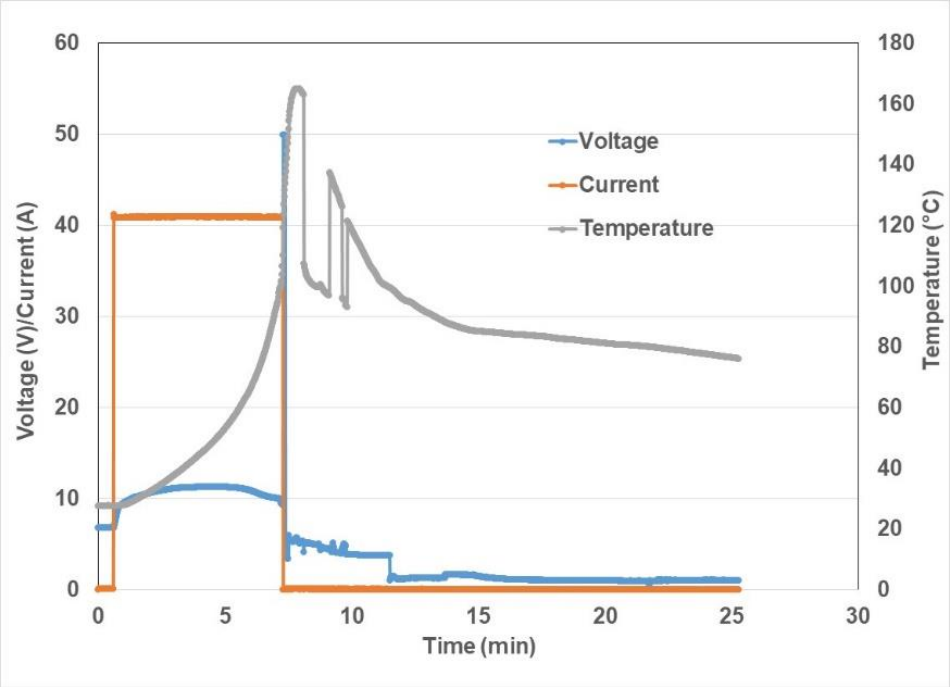

Figure 53. Overcharge test of BL battery

Figure 53 shows the overcharge test for a BL module described above. The voltage dropped at 7.4 minutes and a maximum stack temperature of 165°C was reached at 7.8 min. Seven out of 14 cells vented, and multiple jelly rolls were expelled. Figure 54 shows the module after the test. Figure 55 shows the temperature response on the case exterior during the test. The maximum observed case temperature was 45°C.

Figure 54. Evidence of venting, but no fire, in overcharge test of BL module

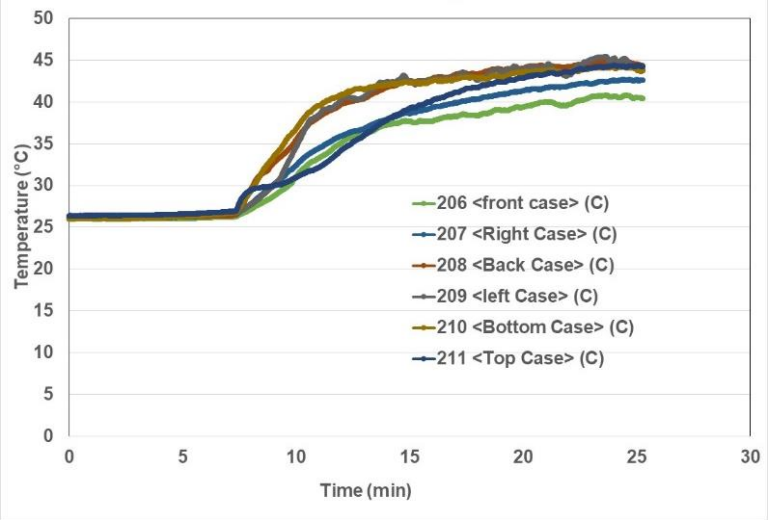

Figure 55. BL battery case temperature during overcharge test

7.2.2 BL and RF Battery External Short Test (Paragraph 2.4.5.2 of DO-311A)

Figure 56 shows the response of an external short circuit test of a BL module. The module was stabilized at 55°C then immediately transferred to a test bunker to perform the external short test. A 2mΩ resistor was used as the external short source. The initial test used an aluminum bus bar that melted due to 1200A being passed through it during the external short test. The aluminum bus bar was replaced with copper to support these high currents. The voltage dropped to 0 V within 1.5 minutes after applying the short, as shown in Figure 56. The stack temperature increased to 302°C in 11 minutes, then began to cool.

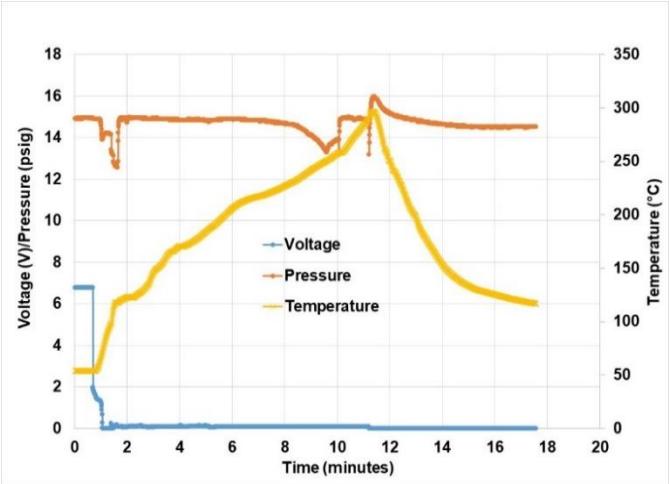

Figure 56. BL battery external short test at 55°C

Figure 57. Evidence of venting and fire, in BL battery from external short test

Figure 57 shows the BL module after the external short test. Seven of the 14 cells vented. There also was evidence of a fire that melted the cell holder.

Figure 58 shows the external short test for a module built with RF electrolyte containing cells, flame-retardant painted case interior, and flame-retardant-coated module wrap. The battery voltage dropped to 0 in 1.3 minutes, corresponding to a short current of 1669A. The temperature of the battery increased for 13 minutes to 245°C, after which it started cooling down.

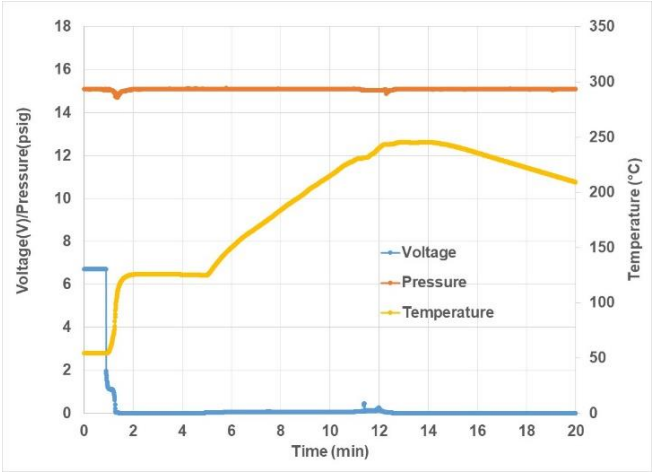

Figure 58. RF battery external short test at 55°C

Figure 59. Evidence of venting, but no fire in RF battery from external short

Figure 59 shows the RF module after the external short test. The stack remained intact and clean with no evidence of fire. There was a leak from a crack on one cell but no signs of violent venting.

7.2.3 BL and RF Battery Overheating Test (2.4.5.5.1 of DO-311A)

A BL module was made with heating wraps around the center cells of both 7P submodules to force overheating. The settings of the power supply used to heat the cells were determined based on previous single-cell overheating tests. Two spark emitters were placed on either end of the cell stack. The center cells propagated heat to the surrounding cells. The increased temperature initiated the exothermic reactions leading to the self-heating of the module. Figure 60 shows that after about 60 minutes of heating the center cell of the BL battery, its voltage dropped, and the stack temperature increased. The heat continued to propagate in both stacks for about 20 minutes. Individual cell venting occurred as the heat propagated during those 20 minutes.

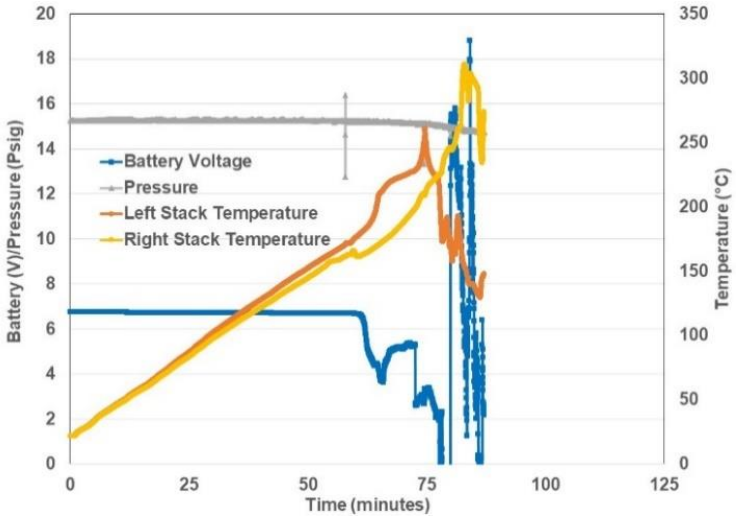

Figure 60. BL battery overheating test

An RF battery was tested by overheating using the same method. Figure 61 shows the first cell(s) vented around 80 minutes after the test was initiated. The voltage decreased at a slower rate compared to the BL module, taking 40 additional minutes for it to drop to 0 V. The maximum

temperature spike happened when the voltage dropped to 0 V. The overheating test demonstrated the slower heat propagation of RF compared to BL, as simulated by the prior ANSYS modeling.

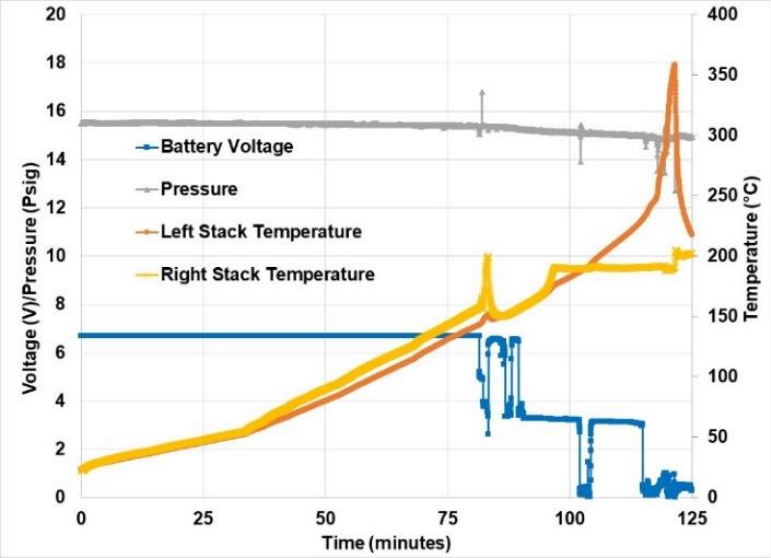

Figure 61. RF battery overheating test

Figure 62 shows the case temperature of the BL and RF modules. The case temperature of the BL module started increasing at 57 minutes and reached a peak at 87 minutes. The BL module therefore demonstrated a propagation time of 30 minutes.

The RF module case temperature started increasing at 82 minutes and reached a peak temperature at 129 minutes, resulting in a propagation time of 47 minutes. The maximum observed case temperature for BL modules was higher (75°C) compared to the RF module (65°C).

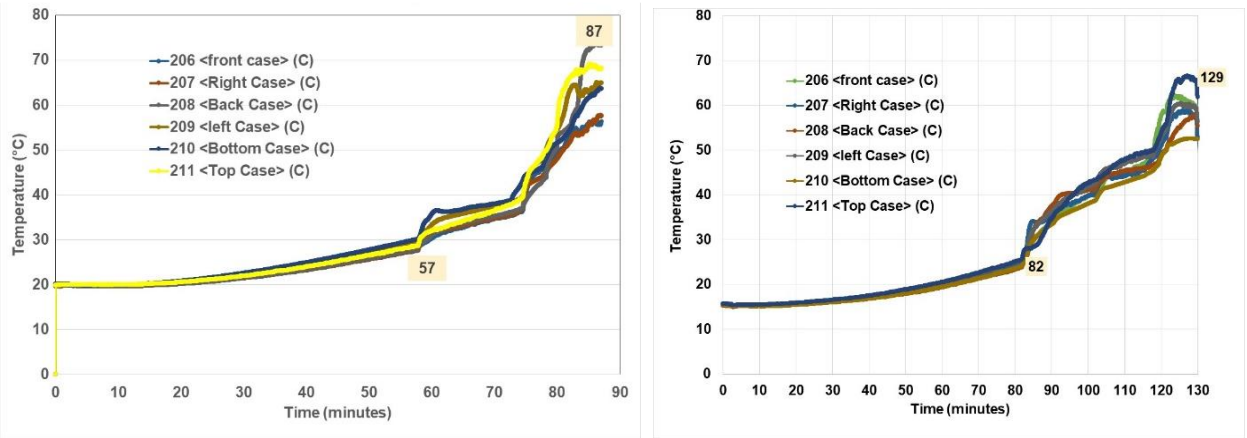

Figure 62. BL (left) and RF (right) battery case temperature

Figure 63 and Figure 64 show the appearance of the modules at the end of the overheating test. The BL module showed strong evidence of burning and was filled with shredded electrodes pointing to severe venting. During the overheating test, 13 out of 14 cells vented in the BL module.

BL battery overheating test
13 of 14 cells vented with evidence of fire

Figure 63. BL battery showed 13 cells venting and burning in overheating test

The RF module did not show any evidence of fire. The inside of the RF battery looked cleaner and only half of the cells vented. These results demonstrate the advantage and improved battery safety of the RF electrolyte combined with the commercial flame-retardant coatings.

RF battery overheating test
7 of 14 cells vented with no evidence of fire

Figure 64. RF battery showed half of the cells intact and no evidence of fire

7.3 SUMMARY

In this task, battery modules were built with and without RF electrolyte and flame-retardant paints and sprays. Safety tests of these modules were performed according to DO-311A. The battery system included all design methods, mitigations, and functional elements required to support a successful qualification regarding DO-311A and DO-160G, as necessary for a future TSO submission (e.g., vent, cell insulation/isolation, etc.). All electronic control hardware and software were omitted from the design to provide a worst-case scenario.

RF and BL cells showed similar capacity, rate capability, temperature capability and cycle life in the capacity, charge acceptance, and high-rate cycle tests.

The overcharge test on the BL module produced venting with expulsion of electrodes. Seven out of the 14 cells vented, although there was no evidence of fire. BL modules subjected to the external short test caused 7 of 14 cells to vent, and the submodule pack melted with evidence of fire. The overheating test caused 13 of 14 cells to vent with enough force to expel and shred electrodes, with evidence of fire.

RF modules were subjected to the same external short and overheating tests noted above. The RF modules incorporated all of the improvements developed in this project to evaluate the effect of the mitigations on safety. Neither the external short nor overheating tests produced fire. While the external short test did not cause cell venting, it did produce a minor surface crack on one cell with electrolyte leakage. The RF module appeared clean when opened; there was no evidence of fire. The overheating test caused 7 out of 14 cells to vent, but with no evidence of fire. Propagation of damage from the heat-taped center cell into other cells in the module was also significantly slower than it was for the BL module. Table 14 summarizes the abuse testing results.

Table 14. Summary of abuse test results of the 7P2S module

Test	Conditions	Results	Appearance after DPA
Overcharge BL (2.4.5.5.1)	40A Overcharge	Vmax 11.3V at 2.5min, Voltage dropped at 7.4min. Max stack temp reached at 7.8 min	7 out of 14 cells vented. Jelly rolls were expelled.
Short Circuit BL (2.4.5.2)	2mΩ short at 55°C	Max stack temp reached at 11min. Max current 1190A. Bus bar melted	One submodule was vented and looked burnt; other submodule did not burn.
Short Circuit RF (2.4.5.2)	2mΩ short at 55°C	Max stack temp reached at 13 min. Max current 1669 A	Looked clean, cells vented a puddle of electrolyte. No fire.
Overheating BL (2.4.5.5.2)	2-3°C/min heating	Initial Voltage drop at 62min. Max stack temp reached at 83 min	All but one (13/14) vented. Multiple jelly rolls expelled, shredded and burnt.
Overheating RF (2.4.5.5.2)	2-3°C/min heating	Initial Voltage drop at 81.5 min. Max stack temp reached at 121.5 min	One-half of submodule was intact (7/14).

The safety advantages of the RF electrolyte and flame-retardant coatings have been demonstrated in the representative battery assembly. This technology shows the clear potential to improve aircraft battery safety.

8. DO-311A OBSERVATIONS AND COMMENTS

With the increased test rigor expected from RTCA DO-311A that now requires whole-battery overcharge or overheat failure tests, and considering the pending release of AC 20-184A requiring all cells to demonstrate thermal runaway, EaglePicher believes that demonstrably beneficial technologies such as RF electrolytes and flame-retardant coatings may be overshadowed by the sought worst-case "end-effect" test results from these forced failure scenarios. As noted within Section 2.4.5.5 of DO-311A, "If a thermal runaway in two or more cells does not occur, the objectives of this testing have not been met. In this case, compliance to this standard would require coordination with the FAA or applicable regulatory agency." This open-ended criterion invokes subjective judgment on the sufficiency of the proposed battery implementation and the included safety mitigations.

Clearly, the discussed evidence contained herein supports the benefit of both the evaluated RF electrolyte, as well as the flame-retardant coatings as part of a broader safety mitigation strategy. The intent of the RF electrolyte is to directly address cell volatility through a reduction of the vapor pressure and flash point while maintaining the intended cell performance. The included data

supports that the resulting thermal response of cells incorporating the RF electrolyte is far less vigorous and demonstrates a reduced likelihood of thermal runaway—this can technically be considered a test failure as the desired end-effect of cell thermal runaway may not be consistently achieved. EaglePicher thus believes that rather than the explicitly required failure demonstrations, the design for any Lithium aviation battery should be based upon the completion of system-level safety and hazard assessments that address primary and secondary failure modes and their effects, not just for the battery and its components (including cells), but also for the interfacing electrical system and supporting mechanical structures that enable the planned battery installation(s). A failure assessment test plan can then be developed specific to the planned battery implementation that will drive necessary failure mitigations and corresponding applicable tests from the "menu" of those outlined within DO-311A to sufficiently support the battery design implementation within the identified airframe(s). This safety-assessment-based design approach mimics that utilized for Lithium rechargeable batteries to be deployed on military aircraft as guided by MIL-PRF-29595A that cites safety and hazard evaluations to be conducted per MIL-STD-882E for a contextually sufficient Lithium-ion battery integration.

9. CONCLUSION

EaglePicher used this opportunity with the FAA to develop technology to mitigate harmful effects of thermal runaway in Li-ion batteries. An RF electrolyte was developed that demonstrated improved stability and reduced heat generation compared to a standard BL Li-ion electrolyte. It also showed little to no flammability when exposed to open flame. Electrical testing demonstrated that the RF electrolyte did not reduce rate capability or cold temperature performance in cylindrical cells.

Abuse tests were conducted on single cells activated with RF and BL electrolyte. The three tests—overcharge, overheating, and short circuit— ended with no RF cells generating fire, whereas many BL cells did. RF cells also had lower maximum skin temperatures overall than the BL cells.

Flame-retardant coatings intended for use on components inside the battery case were evaluated for effectiveness, as well as stability following a one-week storage at 70°C and 90% relative humidity. The coatings were then tested successfully in the presence of LFP 26650 cells undergoing thermal runaway. A paint-based coating was also tested. The flame-retardant paint successfully prevented fire when tested on porous substrate components used in batteries (similar to the flame-retardant sprays), although it was not effective when coated directly on the cell.

Vent characteristics of cells with both electrolytes were used to create an ANSYS model to simulate the expected venting time for RF and BL batteries. The simulation used data generated in this project on both pressure and temperature in cells undergoing thermal runaway. The model predicted a significantly longer time to venting for the RF battery compared to a BL battery. The prediction was later validated in battery tests.

Battery modules having 14 cells in a 7P2S arrangement were fabricated, an RF design incorporating the multiple improvements of this project and a BL design using the initial standard cells with no new battery assembly improvements. The new RF design utilizing reduced flammability electrolyte combined with flame-retardant coatings on internal battery components produced far safer results in DO-311A abuse tests than the standard BL battery design, surviving abuse tests with no evidence of fire.

The RF modules were subjected to the external short circuit and overheating tests since these were the most severe for the BL modules. Maximum temperatures were lower and time to venting was longer than the tested BL batteries in both tests. It was observed after testing that fewer cells vented with no evidence of a fire or burning for both tests.

This project provided encouraging evidence that the safety of Li-ion batteries can be improved through RF electrolytes and flame-retardant materials. Continued refinement of this approach may enable existing and new safety-critical applications for industries such as aircraft and aerospace.

10. REFERENCES

1. S.V. Sazhin, M.K. Harrup and K.L. Gering, J. Power Sources, 196 (2011) 3433-3438.

2. R. Thillaiyan et al, "Electrolyte, a battery including the same, and methods of reducing electrolyte flammability", US Patent Application, Publication number 20160336615, 2015.

3. Judith Jeevarajan, Brad Strangways and Tim Nelson, NASA Battery Workshop, November, 2009.

4. A.W. Golubkov et al, R, RSC Adv., 4 (2014) 3633.

5. L.D. Ellis et al, *J. Electrochem. Soc.*, 164 (2017) A3518-A3528.

6. "Mechanism Leading to Irreversible Capacity Loss in Li ion Rechargeable Batteries", Y. Matsumura, S. Wang and J. Mondori, *J. Electrochem. Soc*., 142 (1995) 2914-2918.

APPENDIX A— TEST METHOD FOR SINGLE CELL THERMAL RUNAWAY VIA OVERCHARGING (2.4.5.4.1 IN DO-311A)

A cell near the center of the battery shall be subjected to overcharging in order to initiate thermal runaway.

a. The EUT shall be serviced and fully charged in accordance with the manufacturer's instructions.

b. Disable all overcharge protective devices connected to the cell that will be tested. Protective devices that are incorporated within the cell shall not be disabled.

c. Select a cell near the center of the battery that will be used to initiate a thermal runaway.

***Note**: For a bank of parallel cells, use a single electrically isolated cell (see point C on Figure 2-2) to initiate a thermal runaway.*

d. Instrument the EUT to measure the temperature of the selected cell, the temperature of the external surface of the EUT, and the temperature of any gases that exit the EUT.

e. Stabilize the EUT at 23°C or the manufacturer's rated maximum operating high temperature, whichever is higher.

f. Connect the selected cell to a power supply set to the following:

   1. voltage limit of at least 1.5 times the nominal cell voltage.
   2. current limit of at least 2 times the I_1 (or I_{Max} if less than I_1) current of the cell.

g. After temperature stabilization, the EUT may be removed from the temperature chamber (if used) to avoid contamination of the chamber. If the EUT is removed from the chamber, step f shall be applied prior to the battery temperature dropping 5°C below the specified stabilization temperature in step e.

h. The power supply may be removed once a thermal runaway has initiated. If a thermal runaway does not initiate within two hours, the power supply may be removed.

i. Continue to monitor the EUT for 16 hours after the power supply has been removed.

j. Throughout the test, record the applied voltage, charging current, cell temperature, EUT external temperature, and the temperature of any gases that exit the EUT.

***Note**: The test sequence should be recorded on video.*

k. Report the following information:

- Identification of the selected cell.
- Rupture of the EUT.
- Emission of gas, smoke, soot, or fluid from the EUT.

- A tabular or graphical representation of the applied voltage, charging current, cell temperature, EUT external temperature, and the temperature of any gases that exit the EUT, as a function of time.

- Protective devices that were not disabled.

- A statement declaring whether thermal runaway did or did not occur in the selected cell.

- If thermal runaway did occur, objective evidence, confirmed by post-test inspection, that the selected cell achieved thermal runaway.

Note: *Examples of "Objective Evidence" may include:*
Melted metallic components of cells
Decomposed active materials
Pyrolyzed (charred) cell contents
Peak cell temperature indicative of thermal runaway (for the tested chemistry)

Verify that the EUT meets the requirements of 2.2.2.3.

APPENDIX B— COMPLIANCE

Based upon the demonstrated performance and safety compliance to the RTCA/DO-311A MOPS as noted within the tables captured below, the pursued safety technologies (RF electrolyte, and FR coatings) improve the robustness of the existing MAR-9563 design implementation. Pursuant to 14 CFR 21.603(a)(1), the MAR-9563 meets the requirements of CFR Title 14 Part 21 Subpart O of TSO-C179b to support certification for flight readiness.

As an existing battery assembly, the MAR-9563 has a demonstrated environmental and safety test capability. The compliance matrix shown in Table 15 summarizes overall compliance to DO-311A. Where the new safety technologies are relevant, appropriate notations are included within the following tables, although the majority of the test context is not directly applicable to the specific scope of this project work for reasons noted earlier. The described safety technologies were pursued with the primary intent of adding margin to an existing design, and to potentially enable more volatile Li-ion electrochemistries for use within commercial aviation.

Table 15. MAR-9563 compliance to DO-311A

Guidelines and / or Requirement	DO-311A Section	Means of Compliance
Battery Categories - 1.4		
Energy Categories	1.4.1	Category 4 is applicable
Venting Categories	1.4.2	Category B is applicable
Architecture Categories	1.4.3	Category “Standalone” is applicable
Regulatory Responsibilities	1.5	Testing and Analysis may be required to obtain installation approval (airframe specific)
Test Procedures	1.6	Test Procedures outlined in DO-311A will be adhered to unless a deviation is requested
Requirements, Guidelines, and Test Procedures - 2		
General Requirements - 2.1		
Fire Protection	2.1.1	Cell Selection & Design
Design Assurance (DAL)	2.1.2	Software will be in accordance with DO-178C
Marking - 2.1.3 (Standalone)	2.1.3.1	Marking and labeling of the MAR-9563 contains the required information per DO-311A, 14 CFR Part 21.616(d) and 45.15(b)(c), and TSO-C179b
General Safety Requirements	2.1.4	Design, Analysis, Testing, and as documented within EP-MM-9563 Rev OR
Battery Protective Features	2.1.4.1	Design
Battery Warning Features	2.1.4.2	Design
Charging and Discharging Protection	2.1.5	Design

Guidelines and / or Requirement	DO-311A Section	Means of Compliance
Overdischarge Protection	2.1.6	Design
Mitigation of Cell Failures	2.1.7	Design
Venting Provisions	2.1.8	Design – Venting Category B is applicable
Shelf Life and Float Life	2.1.9	Design and Appendix B of DO-311A is not being applied at this time. However, EP-MM-9563 Rev OR will specify shelf life and float life recommendations.
Design Guidelines - 2.1.10		
General Guidelines	2.1.10.1	Design, Thermal Analysis, Testing, and results
Cell Balancing	2.1.10.2	Design
State of Health Function	2.1.10.3	Design
State of Charge Function	2.1.10.4	Design
Built-In-Test	2.1.10.5	Design
Parasitic Drain	2.1.10.6	Design
Prevention of Bus Back Charging	2.1.10.7	Design
Electrical Bonding	2.1.10.8	Design
Dissimilar Metals	2.1.10.9	Design
Quality	2.1.11	EP-PDS-2
Configuration Control	2.1.11.1	EP-QC-495 Rev BE
Workmanship	2.1.11.2	EP-QC-6671 Rev B
Maintenance Documentation Guidance	2.1.12	EP-MM-9563 Rev OR
Equipment Requirements - 2.2		
Performance Requirements - 2.2.1		
Physical Examination	2.2.1.1	QTP-1242 Rev A, QTR-1033 Rev OR, and ATP-2125 Rev OR No change is expected with implementation of the new safety technologies.
Acceptance Test Procedure	2.2.1.2	ATP-2125 Rev OR and QTR-1033 Rev OR No change is expected with implementation of the new safety technologies.
Insulation Resistance	2.2.1.3	QTP-1242 Rev A and QTR-1033 Rev OR No change is expected with implementation of the new safety technologies.
Handle Strength	2.2.1.4	QTP-1242 Rev A and QTR-1033 Rev OR No change is expected with implementation of the new safety technologies.
Rated Capacity	2.2.1.5	QTP-1242 Rev A and QTR-1033 Rev OR Evaluation showed similar performance.

Guidelines and / or Requirement	DO-311A Section	Means of Compliance
Capacity at Low and High Temperatures	2.2.1.6	QTP-1242 Rev A and QTR-1033 Rev OR Evaluation showed similar performance.
Constant Voltage Discharge for High Rate Batteries	2.2.1.7	QTP-1242 Rev A and QTR-1033 Rev OR Evaluation showed similar performance.
Charge Acceptance	2.2.1.8	QTP-1242 Rev A and QTR-1033 Rev OR Evaluation showed similar performance.
Charge Retention	2.2.1.9	QTP-1242 Rev A and QTR-1033 Rev OR Not performed within scope of this project.
Cycling of High Rate Batteries	2.2.1.10	QTP-1242 Rev A and QTR-1033 Rev OR Evaluation showed similar performance,
Rapid Discharge at Short-Time Operating High Temperature	2.2.1.11	Not Performed
Short Circuit Protection	2.2.1.12	QTP-1242 Rev A and QTR-1033 Rev OR
Overdischarge Protection	2.2.1.13	QTP-1242 Rev A and QTR-1033 Rev OR
Overcharge Protection	2.2.1.14	QTP-1242 Rev A and QTR-1033 Rev OR
Safety Requirements - 2.2.2		
Short-circuit without Protection	2.2.2.1	QTP-1242 Rev A and QTR-1033 Rev OR Pending – intent to show improved margin with reduced internal battery damage.
Overdischarge without Protection	2.2.2.2	QTP-1242 Rev A and QTR-1033 Rev OR Not performed within scope of this project.
Single Cell Thermal Runaway Containment	2.2.2.3	RF demonstrates a higher margin of safety than BL in single cell overcharge and overheating tests in terms of time to fail, and the resulting failure effects.
Battery Thermal Runaway Containment	2.2.2.4	QTP-1242 Rev A and QTR-1033 Rev OR Pending – intent to show improved margin with reduced internal battery damage.
Explosion Containment	2.2.2.5	QTP-1242 Rev A and QTR-1033 Rev OR
Drop Impact Resistance	2.2.2.6	Not Performed
Equipment Requirements – Environmental Conditions - 2.3		
Temperature	2.3.1	See Appendix 4
Altitude	2.3.1	See Appendix 4
Decompression	2.3.1	See Appendix 4
Overpressure	2.3.1	See Appendix 4
Temperature Variation	2.3.1	See Appendix 4
Humidity	2.3.1	See Appendix 4
Operational Shock	2.3.1	See Appendix 4
Crash Safety	2.3.1	See Appendix 4
Vibration	2.3.1	See Appendix 4

Guidelines and / or Requirement	DO-311A Section	Means of Compliance
Explosive Atmosphere	2.3.1	See Appendix 4
Waterproofness	2.3.1	See Appendix 4
Fluids Susceptibility	2.3.1	See Appendix 4
Sand and Dust	2.3.1	Not Performed
Fungus Resistance	2.3.1	See Appendix 4
Salt Fog	2.3.1	See Appendix 4
Magnetic Effect	2.3.1	See Table 2
Power Input	2.3.1	See Table 2
Voltage Spike	2.3.1	See Table 2
Audio Freq. Conducted Susceptibility	2.3.1	See Table 2
Induced Signal Susceptibility	2.3.1	See Table 2
RF Susceptibility	2.3.1	See Table 2
Emission of RF Energy	2.3.1	See Table 2
Lightning Induced Transient Susceptibility	2.3.1	See Table 2
Lightning Direct Effects	2.3.1	Not Performed
Icing	2.3.1	Not Performed
Electrostatic Discharge	2.3.1	See Table 2
Fire / Flammability	2.3.1	See Table 2
Environmental Test Procedures	2.3.2	QTP-1242 Rev A and QTP 1247 Rev A
Equipment Test Procedures - 2.4		
Equipment Test Procedures	2.4	QTP-1242 Rev A and QTP 1247 Rev A
Definitions of Terms and Conditions of Test	2.4.1	QTP-1242 Rev A and QTP 1247 Rev A
Test Matrix	2.4.2	QTP-1242 Rev A
Test Setup	2.4.3	QTP-1242 Rev A, QTP-1247 Rev A, QTR-1033 Rev OR and QTR-1056 Rev A
Special Grounding Provisions	2.4.3.1	QTP-1242 Rev A and QTR-1033 Rev OR
Performance Test - 2.4.4		
Physical Examination (Paragraph 2.2.1.1)	2.4.4.1	QTP-1242 Rev A and ATP-2125 Rev OR and QTR-1033 Rev OR
Acceptance Test Procedure (Paragraph 2.2.1.2)	2.4.4.2	ATP-2125 Rev OR and QTR-1033 Rev OR
Insulation Resistance Test (Paragraph 2.2.1.3)	2.4.4.3	QTP-1242 Rev A and QTR-1033 Rev OR
Test Method	2.4.4.3.1	QTP-1242 Rev A and QTR-1033 Rev OR
Handle Strength (Paragraph 2.2.1.4)	2.4.4.4	QTP-1242 Rev A and QTR-1033 Rev OR
Test Method	2.4.4.4.1	QTP-1242 Rev A and QTR-1033 Rev OR

Guidelines and / or Requirement	DO-311A Section	Means of Compliance
Capacity Test (Paragraph 2.2.1.5)	2.4.4.5	QTP-1242 Rev A and QTR-1033 Rev OR Pending – initial evaluation showed similar performance
Test Method	2.4.4.5.1	QTP-1242 Rev A and QTR-1033 Rev OR
Capacity Test at Low and High Temperature (Paragraph 2.2.1.6)	2.4.4.6	QTP-1242 Rev A and QTR-1033 Rev OR Pending – initial evaluation showed similar performance
Test Method	2.4.4.6.1	QTP-1242 Rev A and QTR-1033 Rev OR
Constant Voltage Discharge Rate for High Rate Batteries (Paragraph 2.2.1.7)	2.4.4.7	QTP-1242 Rev A and QTR-1033 Rev OR Not performed within scope of this project.
Test Method	2.4.4.7.1	QTP-1242 Rev A and QTR-1033 Rev OR
Charge Acceptance Test (Paragraph 2.2.1.8)	2.4.4.8	QTP-1242 Rev A and QTR-1033 Rev OR Pending – initial evaluation showed similar performance
Test Method	2.4.4.8.1	QTP-1242 Rev A and QTR-1033 Rev OR
Capacity Retention Test (Paragraph 2.2.1.9)	2.4.4.9	QTP-1242 Rev A and QTR-1033 Rev OR Not performed within scope of this project.
Test Method	2.4.4.9.1	QTP-1242 Rev A and QTR-1033 Rev OR
Cycle Test for High Rate Batteries (Paragraph 2.2.1.10)	2.4.4.10	QTP-1242 Rev A and QTR-1033 Rev OR Pending – initial evaluation showed similar performance
Test Method	2.4.4.10.1	QTP-1242 Rev A and QTR-1033 Rev OR
Rapid Discharge Rate at Short-Time Operating High Temperature (Paragraph 2.2.1.11)	2.4.4.11	Not Performed
Test Method	2.4.4.11.1	Not Performed
Short Circuit Test w/Protection Enabled (Paragraph 2.2.1.12)	2.4.4.12	QTP-1242 Rev A and QTR-1033 Rev OR
Test Method	2.4.4.12.1	QTP-1242 Rev A and QTR-1033 Rev OR
Overdischarge Test (Paragraph 2.2.1.13)	2.4.4.13	QTP-1242 Rev A and QTR-1033 Rev OR
Test Method for Standalone Batteries	2.4.4.13.1	QTP-1242 Rev A and QTR-1033 Rev OR
Test Method for Embedded Batteries	2.4.4.13.2	Not Performed
Overcharge Test (Paragraph 2.2.1.14)	2.4.4.14	QTP-1242 Rev A and QTR-1033 Rev OR
Test Method	2.4.4.14.1	QTP-1242 Rev A and QTR-1033 Rev OR
Safety Test	2.4.5	QTP-1242 Rev A and QTR-1033 Rev OR

Guidelines and / or Requirement	DO-311A Section	Means of Compliance
Short Circuit Test of a Cell (Paragraph 2.2.2.1)	2.4.5.1	QTP-1242 Rev A and QTR-1033 Rev OR BL cell showed higher short current 235A (with fire) than RF cell 70A (no fire).
Test Method	2.4.5.1.1	QTP-1242 Rev A and QTR-1033 Rev OR
Short Circuit Test of a Battery without Protection (Paragraph 2.2.2.1)	2.4.5.2	QTP-1242 Rev A and QTR-1033 Rev OR Pending
Test Method	2.4.5.2.2	QTP-1242 Rev A and QTR-1033 Rev OR
Overdischarge w/o Protection (Paragraph 2.2.2.2)	2.4.5.3	QTP-1242 Rev A and QTR-1033 Rev OR Not performed within scope of this project.
Test Method for Standalone Batteries	2.4.5.3.1	QTP-1242 Rev A and QTR-1033 Rev OR
Test Method for Embedded Batteries	2.4.5.3.2	Not Performed
Single Cell Thermal Runaway Containment Test (Paragraph 2.2.2.3)	2.4.5.4	Overcharge and overheating were both performed – see comments below …
Test Method for Single Cell Thermal Runaway via Overcharging	2.4.5.4.1	Initial overcharge test showed higher incidences of fire in BL cells (3/5) than RF cells (0/7).
Test Method for Single Cell Thermal Runaway via Overheating	2.4.5.4.2	Initial overheating showed higher incidences of fire with BL (2/2) vs RF (0/2)
Battery Thermal Runaway Containment Test (Paragraph 2.2.2.4)	2.4.5.5	QTP-1242 Rev A and QTR-1033 Rev OR (can choose either overcharge, or overheat)
Test Method for Battery Thermal Runaway via Overcharging	2.4.5.5.1	QTP-1242 Rev A and QTR-1033 Rev OR Initial testing revealed overheating produced a more notable failure response.
Test Method for Battery Thermal Runaway via Overheating	2.4.5.5.2	Pending
Explosion Containment Test (Paragraph 2.2.2.5)	2.4.5.6	QTP-1242 Rev A and QTR-1033 Rev OR Container integrity test expected to be similar as BL battery.
Test Method	2.4.5.6.1	QTP-1242 Rev A and QTR-1033 Rev OR
Drop Impact Test (Paragraph 2.2.2.6)	2.4.5.7	Not Performed
Installation Considerations - 3		
Manufacturer Considerations - 3.1		
Aircraft Warning System	3.1.1	Design
Aircraft Environment	3.1.2	Design

Guidelines and / or Requirement	DO-311A Section	Means of Compliance
Installation Considerations - 3.2		
Hazardous Battery Emissions	3.2.1	Design
Installation Design	3.2.2	QTR-1033 Rev OR and QTR-1056 Rev A
Additional Considerations for Installed Equipment	3.2.3	Design and EP-MM-9563 Rev OR
Test Procedures for Installed Equipment	3.3	No Requirement
Appendix		
Safety Guidelines for Users of Rechargeable Lithium Batteries	Appendix A	EP-MM-9563 Rev OR
Optional Test Methods	Appendix B	Not Used
Alternate Test Method for Battery Thermal Runaway	Appendix C	Not Used
RTCA DO-311A Dissenting Opinion Letter	Appendix D	No Requirement
Response to Dissent	Appendix E	No Requirement

The test criteria for the electrical and safety tests were applied based on the recommendations in the Qualification Test Procedure, document QTP-1242 rev C.

Table 16. EMI/EMC qualification

RTCA/DO-160G Requirements	EMI/EMC Qualification Status
Magnetic effect Section 15 Para. 15.3 (Category Z)	QTP-1247 Rev A and QTR-1056 Rev A
Power Input Section 16 Paras. 16.7.5, 16.7.7, (Category Z, R, and I)	QTP-1247 Rev A and QTR-1056 Rev A
Voltage Spike Section 17, Para 17.4 (Category A)	QTP-1247 Rev A and QTR-1056 Rev A
Audio Frequency Conducted Susceptibility Section 18. Pg. 18-7, Figure 18-3 Frequency range: 0 to 148.5936kHz. (Category Z)	QTP-1247 Rev A and QTR-1056 Rev A
Induced Signal Susceptibility Section 19 Paras. 19.3.1-19.3.5	QTP 1247 Rev A and QTR-1056 Rev A

(Category ZC, Table 19-1).	
Conducted Susceptibility Section 20, Para 20.4d (Category Y)	QTP-1247 Rev A and QTR-1056 Rev A
Radio frequency susceptibility Section 20, Para. 20.5d Radiated susceptibility (Category G)	QTP-1247 Rev A and QTR-1056 Rev A
Emission of Radio Frequency Energy Section 21, Para 21.5, 21.6 (Category M)	QTP-1247 Rev A and QTR-1056 Rev A
Lightning Induced Transient Susceptibility Section 22, Para. 22.5 (Category B4, K4, and L4)	QTP-1247 Rev A and QTR-1056 Rev A
Electrostatic Discharge Section 25, Para. 25.5.6 (Category A)	QTP-1247 Rev A and QTR-1056 Rev A

APPENDIX C— HAZARD ANALYSIS

The following documents the design hazards and mitigations of the representative battery assembly during abuse tests following the outline from DO-311A. Li-ion batteries are known to provide reduced weight and volume; the design strikes a balance between minimizing weight/volume and providing the required protection mechanisms to ensure safe operation over a long period. The System Functional Hazard Assessment (S-FHA) was generated for a two-battery configuration and a single battery configuration, summarized in Table 17. The test plan will be used to target an airframe for subsequent laboratory ground testing.

The battery will be tested per RTCA DO-311A and AC20-184 (9) special conditions with the exception of those tests that will have to be assessed at the aircraft installation level: to mitigate the Minimum Operational Performance Standards (MOPS) catastrophic hazards outlined in the S-FHA. While there are multiple safety tests required to show compliance for loss of battery output, there is only one test for thermal containment. Table 18 shows which qualification tests will be performed pertaining to each cascading condition that could lead and or contribute to a catastrophic condition in dual generator failures. Testing will be performed per QTP-1242 MAR-9563 Li-ion Battery Qualification Test Procedure.

Table 17. System Functional Hazard Assessment (S-FHA)

Two Battery Configuration - S-FHA						
S-FHA REF	**Failure Condition**	**Operational Condition**	**Effect on Airplane or Personnel**	**Class**	**Remarks**	**Verification**
1.01.04		Flight, and loss of both generated power sources	Single Battery cannot provide sufficient power for 60 minutes to equipment essential for safe flight and landing.	CAT	Amdt 62 of 14 CFR, Section 23.1353 (h)	FTA 1.01.04 “Loss both generated power sources” = 1E1. per hour
1.02.04		Flight, and loss of both generated power sources	Complete loss of Electrical Power - “Dark airplane”. Loss of all electrical power to equipment essential for safe flight and landing.	CAT		FTA 1.02.04 -
2.02	Either Battery	Flight	Fire may affect other systems,	CAT		FTA 2.02 -

	overheats unprotected, fire not contained		damage structure and may spread to other parts of airplane.			DO-311A [10] tests show containment
Single Battery Configuration - S-FHA						
S-FHA REF	**Failure Condition**	**Operational Condition**	**Effect on Airplane or Personnel**	**Class**	**Remarks**	**Verification**
2.02	Single Battery overheats unprotected, fire not contained	Flight	Fire may affect other systems, damage structure and may spread to other parts of airplane.	CAT		FTA - DO-311A [10] tests show containment

Table 18. S-FHA qualification tests for cascading faults

S-FHA REF	Condition in Dual Generator Failures with Two Batteries	Cascading Faults – QTP-1242 Testing	Test Plan and Rationale
1.01.04 1.02.04	Loss of Battery output either Battery; Flight Loss of Battery output both Batteries	5.8 Short Circuit Test of a Battery without Protection (DO-311A Section 2.4.5.2)	2.4.5.2 is included in test plan.
		5.9 Short Circuit Test of a Cell (DO-311A Section 2.4.5.1)	2.4.5.1 is included in test plan for the cells and is completed.
		5.11 Overdischarge Test without Protection (DO-311A Section 2.4.5.3)	Not included in test plan. Not expected to be most catastrophic failure mode to demonstrate the safety improvements.
		6.26 Explosion Containment Test (DO-311A Section 2.4.5.6)	Not included in test plan. Not needed for technology demonstration on representative module. This is pertinent to a full battery.

2.02	Either Battery overheats, unprotected, fire not contained; Flight	6.19 Battery Thermal Runaway Containment Test (DO-311A Section 2.4.5.5)	2.4.5.5.1 and 2.4.5.5.2 included in test plan for baseline first. RF test will be done with the most severe test.
S-FHA REF	**Condition in Dual Generator Failures with Single Battery**	**Cascading Faults – QTP-1242 Testing**	
2.02	Single Battery overheats, unprotected, fire not contained; Flight	6.19 Battery Thermal Runaway Containment Test (DO-311A Section 2.4.5.5)	2.4.5.5.1 and 2.4.5.5.2 included in test plan for baseline first. RF test will be done with the most severe test.

APPENDIX D— MAR-9563 ENVIRONMENTAL TEST RESULTS

As an existing battery assembly, the MAR-9563 has a demonstrated environmental and safety test capability. The compliance matrix for the environmental qualification is shown in Table 19. The improvement to the existing MAR-9563 battery in terms of the incorporated RF electrolyte and flame-retardant coatings does not cause a significant change in the cell or battery construction. Moreover, the method of integration of the mitigation technologies is not expected to cause a significant change in the weight or volume of the battery. Therefore, the environmental test results of the safer battery are expected to be similar to prior results of the MAR-9563 battery.

Table 19. Environmental qualification

RTCA/DO-160G Environmental Condition Requirements	Qualification Status
As a part of **Temperature and Altitude** Section 4, Para. 4.5.1 and 4.5.2 (Category F1) Operating Low Temp.: = -20°C. Short Time Low Operating Temp = -40C Ground Survival Low Temp.: -55C	QTP-1242 Rev A and QTR-1033 Rev OR
As a part of **Temperature and Altitude** Section 4, Para. 4.5.3 and 4.5.4 (Category F1) Operating High Temp.: = +55°C. Short Time Operating High Temp.=+70C Ground Survival High Temp.: +85C	
In-Flight Loss of Cooling Section 4, Para 4.5.4 (Category X)	No Test Performed
Altitude Section 4, Para. 4.6.1 (Category F1). Altitude = 55,000 ft.	QTP-1242 Rev A and QTR-1033 Rev OR
Decompression Section 4, Para. 4.6.2 (Category F1)	QTP-1242 Rev A and QTR-1033 Rev OR
Overpressure Section 4, Para. 4.6.3 (Category F1) Overpressure Altitude = -15,000 ft. (24.6 psia)	QTP-1242 Rev A and QTR-1033 Rev OR
Temperature Variation Section 5, Para. 5.3.3 (Category S2) Operating Low Temp.: = -20°C. Operating High Temp.: = +55°C.	QTP-1242 Rev A and QTR-1033 Rev OR:

RTCA/DO-160G Environmental Condition Requirements	Qualification Status
Humidity Section 6, Para. 6.3.2 (Category B) **Severe Humidity Environment**, up to RH 95% ±4, +65C ±2, 10 Cycles, 240 hrs. exposure	QTP-1242 Rev A and QTR-1033 Rev OR
Shock Section 7, Para 7.2.1 and 7.3 (Category B) Helicopters and All Fixed Wing **Operational Shock**: 6g, 11 msec. **Crash Safety Shock**: 20g, 11 msec.	QTP-1242 Rev A and QTR-1033 Rev OR
Vibration Section 8, Para. 8.2.1.2 and 8.8.3 (Category U2, Curve F and F1) Random; performance at beginning to end of test period (minimum of 10 min) 3 hours at Endurance Level/repeat in all 3 axis	QTP-1242 Rev A and QTR-1033 Rev OR
Explosive Atmosphere Section 9, Para. 9.6.2 (Category E)	QTP-1242 Rev A and QTR-1033 Rev OR
Waterproofness Section 10, 10.3.1 (Category Y) - Condensing Waterproof	QTP-1242 Rev A and QTR-1033 Rev OR
Fluid Susceptibility Section 11, 11.4.1 (Category F) Test Fluids to be tested: De-Icing Fluid Types I and IV (De-Icing Fluid Category) Isopropyl Alcohol (Solvents and Cleaning Fluids Category) Jet A Fuel (Fuels Category) Phosphate Ester-based (Synthetic) Hydraulic Fluid, Type IV (Hydraulic Fluid Category)	QTP-1242 Rev A and QTR-1033 Rev OR
Sand and Dust Section 12 (Category X)	No Test Performed
Fungus Resistance Section 13, Para. 13.5 (Category F)	QTP-1242 Rev A and QTR-1033 Rev OR

RTCA/DO-160G Environmental Condition Requirements	Qualification Status
Salt Fog Section 14, Para 14.3.6.6 Performance for normal fog (Category S)	QTP-1242 Rev A and QTR-1033 Rev OR
Lightning Direct Effects Section 23 (Category X)	No Test Performed
Icing Section 24 (Category X)	No Test Performed
Fire, Flammability Section 26, Para. 26.6.2.6 (Category C)	QTP-1247 Rev A and QTR-1056 Rev A

Fire, Flammability testing will comply with 14 CFR 25/27/29.853 (a) and 14 CFR 23.2325 (a)(b)(d)